

# **SECOND LAW ANALYSIS OF A COMPRESSION–ABSORPTION HEAT PUMP**

**2007-2008**

## **CERTIFICATE**

This is certified that the minor project report entitled “” is the work of **RUBY SARAN**, University Roll No. 10236 , a student of Delhi College of Engineering. This work was completed under my direct supervision and guidance and forms a part of the Master of Engineering (mechanical) course and curriculum. She has completed his work with utmost sincerity and diligence.

The work embodied in this minor project has not been submitted for the award of any other degree to the best of my knowledge.

# CONTENTS

<b>CERTIFICATE</b>	<b>I</b>
<b>ACKNOWLEDGEMENT</b>	<b>II</b>
<b>ABSTRACT</b>	<b>III</b>
<b>NOMENCLATURE</b>	<b>IV</b>
<b>LIST OF FIGURES</b>	<b>VII</b>
<b>LIST OF TABLES</b>	<b>IX</b>
<b>1. INTRODUCTION</b>	<b>1</b>
Historical background	1
Features of a compression-absorption system	1
Introduction to first and second law analysis	3
Scope of the work	4
<b>2. LITERATURE REVIEW</b>	<b>5</b>
Lorenz cycle	5
Compression-absorption cycle on a p-T-x diagram	6
Different types of compression-absorption system	8
Single stage compression-absorption system	
Two stage compression- absorption system	
Desorber-absorber heat exchange cycle	
Different schedules of compression-absorption system	10

compression-absorption system with compressor between absorber and desorber	
compression-absorption system with mechanical vapour compression between low and high pressure level of a sorption heat pump	
sorption-compression heat pump with low pressure booster	
sorption-compression heat pump with high pressure booster	
Theoretical thermodynamic studies reported in the literature	13
Conclusion	17

### **3. THERMODYNAMIC ANALYSIS OF A COMPRESSION-ABSORPTION**

#### **SYSTEM 18**

Description of a single stage compression-absorption system	18
Assumptions taken into consideration for the analysis	19
p-T-x relations for the ammonia-water mixture	20
First law analysis	21
Governing equations based on first law analysis	
Terminology and performance parameters related to first law analysis	
Second law analysis	26
Governing equations based on second law analysis	
Terminology and performance parameters related to second law analysis	

### **4. PROBLEM FORMULATION AND SOLUTION METHODOLOGY 31**

Problem Formulation	31
Solution Methodology in EES	31
Computer Program and its Output	33

Performance Calculations	33
<b>5. RESULTS AND DISCUSSION</b>	<b>37</b>
5.1 Operating Conditions	37
5.2 Results of First Law Analysis	38
5.3 Results of Second Law Analysis	44
5.4 Analysis of High Temperature Lift Compression-Absorption heat pump	55
<b>6. CONCLUSIONS</b>	<b>58</b>
<b>APPENDIX I</b>	<b>60</b>
<b>REFERENCES</b>	<b>65</b>

# LIST OF FIGURES

## Chapter 2

- Fig. 2.1 T-s diagram representing the processes in a Lorenz cycle 5
- Fig. 2.2 p-T-x diagram of a compression-absorption system 7
- Fig. 2.3.1 Schematic diagram of a single stage compression-absorption system 8
- Fig. 2.3.2 Schematic diagram of a two stage compression-absorption system 9
- Fig. 2.3.3 Desorber- absorber heat exchange cycle 10
- Fig. 2.4.1 Compression-absorption system with compressor between absorber and desorber 11
- Fig. 2.4.2 Compression-absorption system with mechanical vapour compression between low and high pressure level of a sorption heat pump. 11
- Fig. 2.4.3 Compression-absorption system with low pressure booster 12
- Fig. 2.4.4 Compression-absorption system with high pressure booster 13

## Chapter 3

- Fig. 3.1 Schematic diagram of a compression-absorption system 28

## Chapter 5

- Fig. 5.2.1 Variation of coefficient of performance with absorber temperature 38
- Fig. 5.2.2 Variation of coefficient of performance with compressor efficiency 39

Fig. 5.2.3	Variation of coefficient of performance with heat exchanger effectiveness	40
Fig. 5.2.4	Variation of compressor input power with absorber temperature	41
Fig. 5.2.5	Variation of circulation ratio with absorber temperature	42
Fig. 5.2.6	Variation of concentration difference with absorber temperature	43
Fig. 5.3.1	Variation of exergetic efficiency with absorber temperature ( $T_d = 30^\circ\text{C}, 35^\circ\text{C}, 40^\circ\text{C}$ )	45
Fig. 5.3.2	Variation of exergetic efficiency with heat exchanger effectiveness ( $T_d = 30^\circ\text{C}, 35^\circ\text{C}, 40^\circ\text{C}$ )	46
Fig. 5.3.3	Variation of exergetic efficiency with compressor efficiency	47
Fig. 5.3.4	Variation of exergy destruction ratio in the absorber with absorber Temperature	48
Fig. 5.3.5	Variation of exergy destruction ratio in the compressor with absorber Temperature	49
Fig. 5.3.6	Variation of exergy destruction ratio in the compressor with Compressor efficiency	50
Fig. 5.3.7	Variation of exergy destruction ratio in the desorber with absorber Temperature	51
Fig. 5.3.8	Variation of exergy destruction ratio in the expansion valve with absorber temperature	52
Fig. 5.3.9	Variation of exergy destruction ratio in the expansion valve with Heat exchanger effectiveness	53
Fig. 5.3.10	Variation of exergy destruction ratio in the solution pump with absorber temperature	54

Fig. 5.3.11 Variation of exergy destruction ratio in the solution heat exchanger	
With absorber temperature	55
Fig. 5.4.1 Variation of COP with absorber temperature	56
Fig. 5.4.2 Variation of COP with compressor efficiency	57

## LIST OF TABLES

Table I:	Thermodynamic properties used for exergetic calculations for the NH <sub>3</sub> -H <sub>2</sub> O mixture at various state points of the cycle. (R=5, T <sub>d</sub> = 30°C)	60
Table II:	Exergy loss rates of the various components of the system (T <sub>a</sub> =60°C, T <sub>d</sub> = 30°C, R=5)	60
Table III:	Heat transfer rates of components and performance parameters of the system.	61
Table IV:	Variation of coefficient of performance with compressor efficiency at various desorber temperatures (T <sub>a</sub> =60°C, ε =0.7)	61
Table V:	Exergetic efficiency for various compressor efficiencies.	62
Table VI:	Exergy destruction ratios of all the components expressed as percentages at various absorber temperatures.	62
Table VII:	Exergy destruction ratio of the compressor with absorber temperature at various compressor efficiencies.	63
Table VIII:	Exergy destruction ratio of the absorber with absorber temperature. (T <sub>d</sub> =30°C, 35°C, 40°C)	63



Table IX:	Exergy destruction ratio of the desorber with absorber temperature. ( $T_d = 30^\circ\text{C}, 35^\circ\text{C}, 40^\circ\text{C}$ )	64
Table X:	Exergy destruction ratio of the solution pump with absorber temperature. ( $T_d = 30^\circ\text{C}, 35^\circ\text{C}, 40^\circ\text{C}$ )	64
Table XI:	Exergy destruction ratio of the expansion valve with absorber temperature. ( $T_d = 30^\circ\text{C}, 35^\circ\text{C}, 40^\circ\text{C}$ )	65
Table XII:	Exergy destruction ratio of the solution heat exchanger with absorber temperature. ( $T_d = 30^\circ\text{C}, 35^\circ\text{C}, 40^\circ\text{C}$ )	65

## **ABSTRACT**

The objective of this project is to review and analyse a compression-absorption heat pump of 100 kW heating capacity to be operated at various parameters like absorber temperature varying in the range of 50-80°C, desorber temperature varying from 30-40°C and the compression ratios of 5 and 6 . The working fluid selected is the ammonia-water mixture. A computer program has been developed in the Engineering Equation Solver (EES) software to carry out a detailed first and second law analysis of the system and the various performance parameters like the coefficient of performance (COP), circulation ratio (CR), exergetic efficiency etc. are calculated. The mass, material and energy balance equations are written for all the components of the system. The thermodynamic state of each of the points within the cycle is calculated . A detailed picture of the system is provided by the results of exergy analysis. The exergy analysis emphasizes that both losses and irreversibility have an impact on system performance. The exergy loss of each component and the dimensionless total exergy loss are calculated. The results show that the largest exergy loss occurs in the absorber, followed by compressor, desorber and expansion valve. Exergy losses in the pump and solution heat exchanger are small compared to other components.

Consequently, the results of the second law analysis can be used to identify the less efficient components of the system.

## NOMENCLATURE

<b>Abbreviations/ Symbols</b>	<b>Description</b>
COP	Coefficient of performance
CR	Circulation ratio
EDR	Exergy Destruction Ratio
R	pressure ratio
h	enthalpy (kJ/kg)
s	entropy (kJ/kgK)
v	specific volume (m <sup>3</sup> /kg)
m	mass flow rate (kg/s)
CAHP	Compression-Absorption heat pump
DAHX	Desorber absorber heat exchange
EES	Engineering Equation Solver
Q	heat load (kW)
T	temperature (K)
P	pressure (bar)
x	concentration (kg/kg)
W	Work (kW)
C	Celcius
p-T-x	pressure-Temperature-concentration
NH <sub>3</sub>	ammonia

H<sub>2</sub>O            water

°                degree

### **Greek Symbols**

Δ                Change

η                Efficiency

ε                Effectiveness

Σ                Summation

ψ                Exergy

δ                Efficiency defect

### **Subscripts**

0                Dead state

ex               exergetic

p                pump

shx             solution heat exchanger

a                absorber

d                desorber

ev               expansion valve

c                compressor

in               inlet stream

out              outlet stream

*m,r*             mean temperature of heat rejection

<i>m,d</i>	mean temperature of heat addition
<i>d</i>	discharge
<i>s</i>	suction
ss	strong solution
ws	weak solution
<i>m</i>	minimum
<i>GA</i>	absorber glide
<i>GD</i>	desorber glide
add	addition
rej	rejection
tot	total

# INTRODUCTION

## 1.1 Historical Background

With a view to search for a system which can be used for high temperature lift at lower pressure ratios without using the harmful ozone depleting refrigerants such as the chlorofluorocarbons (CFCs) as used in the conventional vapour compression systems, a novel system called the compression-absorption system was developed in 1895 by Osenbrueck, which became a German patent. Later in 1950, the idea of combining a compressor to an absorption system was presented by Altenkirch. Among the heat pump technologies, absorption/compression cycles are suitable for large temperature lifts and high temperature applications. Furthermore, non-conventional sources of energy such as solar, waste heat, and geothermal can be used as their primary energy input. This system is a hybrid of the conventional vapour compression and absorption systems which possess best features of both the types. Many industrial processes have heating demands in the temperature range of 75-100°C. At the same time, waste heat holding typically a temperature of 30-50°C is available. The limitation in heat pump alternatives for temperatures around 100°C after the high temperature refrigerant CFC-114 was abandoned, has turned the focus on alternative heat pump processes using natural working fluids. Efficient heat pumping technologies like compression-absorption systems are therefore attractive in order to reduce the specific energy consumption. Such systems are gaining popularity because they operate on environment friendly refrigerants conforming Montreal and Kyoto protocols.

## 1.2 Features of a Compression-Absorption System

The compression-absorption systems can be operated over a wide range of temperatures, between -10 and 160°C, using ammonia-water as the working fluid and with pressures not exceeding 20 bar (Stokar and Trepp, 1986). These systems utilize the available low temperature waste heat sources thus providing high temperature lifts required in many industrial applications such as pasteurization, dairy technology and steam production etc.

This system operates on a refrigerant-absorbent mixture unlike the vapour compression system which uses a pure refrigerant fluid. A key advantage of the compression-absorption cycle is the extended range of temperatures available for a mixture compared to pure refrigerants. This is the effect of reduced vapour pressure obtained for a refrigerant in a mixture with a less volatile component. Therefore, refrigerants which, as pure components, are restricted by too high pressures at the required temperatures can be used over new temperature ranges. One example is  $\text{NH}_3$  which has a saturation pressure of 25 bar at  $58.2^\circ\text{C}$ . When mixed with  $\text{H}_2\text{O}$  it could be possibly be used upto  $150\text{-}160^\circ\text{C}$  at similar pressures. Thus, by using mixtures, it is possible to cover temperature regimes where it is difficult to find a suitable pure refrigerant [1]. An ammonia-water mixture is a non ideal mixture which possesses more than Raoult's law of stability. Mixing of ammonia and water is accompanied by the absorption of heat. Ammonia-water mixture is suitable for high temperature heat pump applications because of the reduced pressure when working at higher temperatures. This non-azeotropic mixture has therefore been chosen for the present study.

Another advantage of this cycle is the gliding temperature profiles obtained in the absorber and desorber. Gliding temperature here refers to the temperature change obtained as the volatile component is absorbed into or evaporated out of the solution. Within the given temperature limits of the heat source and sink there is a considerable freedom of placing the solution field within the corresponding saturation pressures of the pure solute and solvent. This characteristic feature provides greater design flexibility than is possible for single fluid heat pumps. By a suitable choice of the concentration range external conditions can be optimally matched to the properties of the working pair and the heat pump components. Desorption and absorption processes follow non-isothermal paths at constant , but different pressures due to the fact that bubble points of the desorbing and the resorbing solution change as the concentration of the refrigerant lessens or increases respectively. This behaviour can be utilized to reduce exergy losses by counter current heat exchange when non-isothermal heat sources and sinks are available such as ground water and district heating water.

By using a compression-absorption cycle instead of a single fluid compression cycle at identical temperature levels, the process pressure levels are reduced. Depending on the

thermodynamic properties of the refrigerant-solution the pressure ratio may become smaller which favourably affects compressor lifetime [1]. Compared with a single-fluid compression cycle, the performance of the compression/absorption cycle is improved as the external temperature gradients increase. Although the compression/absorption cycle is usually only put forward as an alternative to compression cycles for applications involving large external temperature gradients, this study has shown that this cycle is also interesting for applications where the external temperature gradients are small. The more isothermal the conditions are, however, the greater is the need to optimize the parameters within the cycle in order to maximize its performance. From the results presented in this thesis it is clear that the compression/absorption heat pump cycle offers several advantages over other types of heat pumps. In many cases it gives a higher or equally high COP compared with the single-fluid compression heat pump but also the smaller SCD (i.e. size of the compressor) found for this cycle is an advantage. .

### **1.3 Introduction to First and Second Law Analysis**

The first law analysis is the most commonly used method to evaluate the performance of any thermodynamic system. Extensive work has been reported on energy related analysis of devices, technologies and systems, in a variety of fields. First law analysis of a compression-absorption system has been done by many researchers including George et al (1989), Arun et al (1999) Pratihari et al (2001), etc. But the design and analysis based only on the first law is not sufficient. The first law analysis involves application of mass, material and energy balances on the components of the system. The first law is concerned only with the conservation of energy, it gives no information on how, where, and how much the system performance is degraded. In recent years, there has been a growing interest in the use of principles of second law of thermodynamics for analyzing and evaluating the thermodynamic performance of thermal systems. The first law optimization should result in maximizing the coefficient of performance (COP), thus providing maximum heat removal for minimum power input, while the second law optimization should result in maximizing the exergetic efficiency.



First law analysis of compression-absorption system has been carried out by several researchers, however very less work has been reported on second law analysis of this system. Compared to the energy analysis, the exergy analysis can better and accurately show the location of inefficiencies in a system. A typical thermal design based on the first law of thermodynamics allows us to address issues related to the energy balance of the system. Exergy (or availability) analysis is a powerful tool in the design, optimization and performance evaluation of energy systems. This analysis can be used to identify the main sources of irreversibility (exergy loss) and to minimize the generation of entropy in a given process where the transfer of energy and material take place. Exergy analysis is an effective thermodynamic scheme for using the conservation of mass and energy principles together with the second law of thermodynamics for the design and analysis of thermal systems, and is an efficient technique for revealing whether or not and by how much it is possible to design more efficient thermal systems by reducing the inefficiencies. Several theoretical and experimental studies based on exergy concept with vapour compression and vapour absorption heat pump systems have been published but the studies on exergy analysis of compression-absorption systems are relatively few. The results from exergy analysis can also be used to access and optimize the performance of a hybrid vapour compression-absorption system.

#### **1.4 Scope of the Work**

In the present work, a comprehensive study and a detailed first and second law analysis of a compression-absorption system has been done for its use in high temperature applications. A computer program has been developed in the Engineering Equation Solver software to evaluate the performance of the system for a particular set of operating conditions. The effects of varying these parameters on the system performance has also been studied. The irreversibilities in different components of the system have been computed and their contribution to the total exergy loss of the system has been studied with a view to improve those components whose contribution are significant.

## LITERATURE REVIEW

A thorough review of literature has been carried out to understand the basic concepts and to explore the theoretical work carried out on compression-absorption systems. Although the basic ideas are old, the technique is new, and hence an understanding of the concepts involved with a few clarifying explanations is required to comprehend the system under study. A brief account of the same has been presented in this chapter.

### 2.1 Lorenz Cycle

In contrast to the Carnot cycle, which is the ideal thermodynamic cycle for the conventional mechanical heat pumps, the ideal thermodynamic cycle for a compression-absorption heat pump using a zeotropic mixture like ammonia-water mixture is called the Lorenz cycle. In other words, the Lorenz cycle can be assumed as an ideal reference in place of a reverse Carnot cycle. The Lorenz cycle is shown in Fig. 1. It consists of four processes which are represented in the T-S diagram shown below.

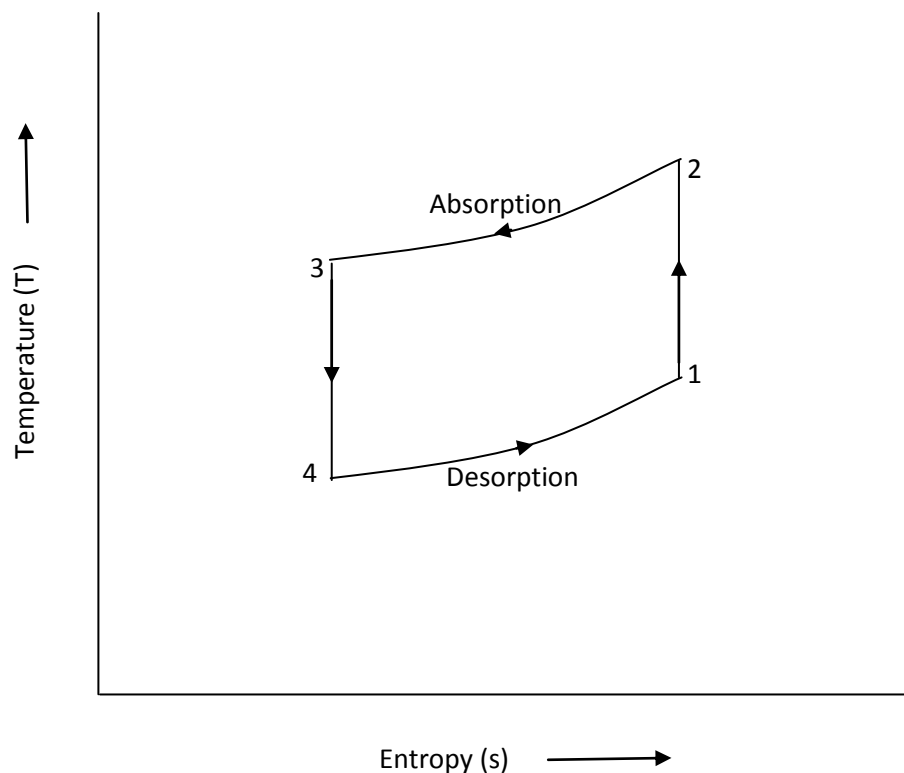


Fig. 2.1. T-s diagram representing the processes in a Lorenz cycle

The process 1-2 is the isentropic compression process taking place in the compressor. After the compression process, in the process 2-3, the heat rejection takes place at a constant pressure but the temperature of the working fluid decreases as the concentration of the solution increases. It is followed by the isentropic expansion process occurring from 3-4. The last process which completes the cycle is heat addition process taking place from 4-1 when the temperature of the fluid increases at a constant pressure. The energy transfer in a Lorenz cycle are as follows:

1. Heat rejection( $Q_r$ )=  $(T_0 + \frac{\Delta T}{2})(s_2 - s_3)$
2. Heat addition ( $Q_d$ )=  $(T_r - \frac{\Delta T}{2})(s_1 - s_4)$
3.  $W_{net} = Q_d - Q_r$

The COP of a Lorenz cycle can be expressed as:

$$COP_{lorenz} = \frac{T_{m,r}}{T_{m,r} - T_{m,d}}$$

where,  $T_{m,r}$  = mean temperature of heat rejection

$T_{m,d}$  = mean temperature of heat addition.

Lorenz cycle is considered to be more realistic representation of actual working processes as it takes into account the temperature gradients during absorption and desorption processes. The Lorenz cycle has a smaller refrigerating effect than the Carnot cycle and more work is required. However, this cycle is more practical to use than the Carnot cycle when a refrigeration system operates between two single phase fluids such as air or water. It is observed that the entropy change for the Lorenz cycle is larger than for the Carnot cycle at the same temperature levels and the same capacity i.e., the heat rejection is larger and work requirement is also larger for the Lorenz cycle.

## 2.2 Compression-Absorption Cycle on a p-T-x diagram

A cycle working with a binary mixture like ammonia-water is represented on the p-T-x diagram as represented in Fig. 2.2.

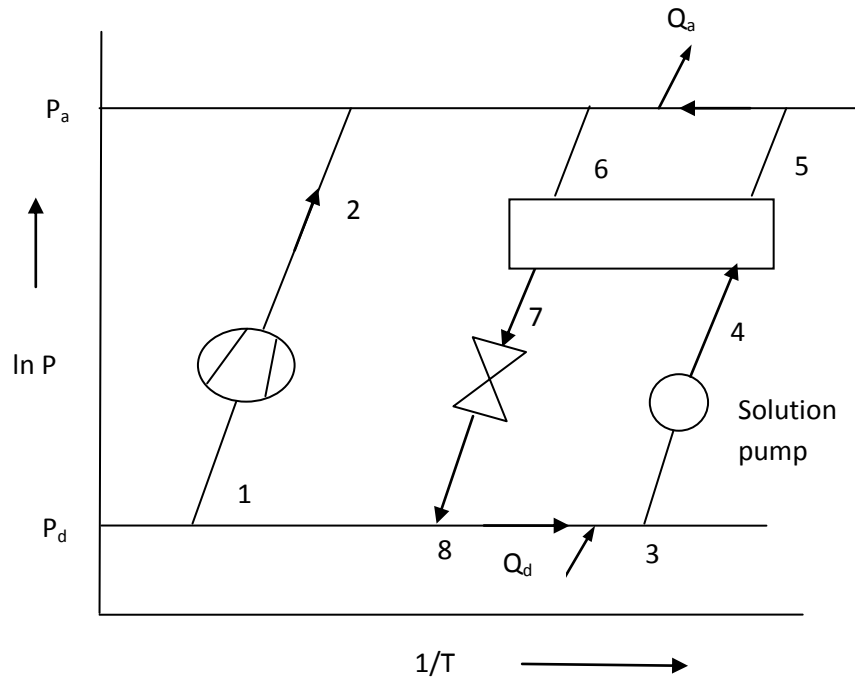


Fig. 2.2 p-T-x diagram of a compression-absorption system

In the above figure,  $P_d$  is the desorber pressure which corresponds to the lower pressure of the system. Pressures at points 1,3 and 8 are same.  $P_a$  is the higher pressure of the system. The pressures at points 2, 6, 7, 4, 5 are same and equal to absorber pressure.

In the absorber, high-pressure superheated ammonia discharge vapour is absorbed by the low concentration solution that is called weak solution. This absorption process is an exothermic reaction during which the concentration of solution increases and there is a decrease in absorber temperature at a constant absorber pressure. This is called as **gliding temperature profile** of the absorber. The path 6-7-8 represents strong solution path and the concentration at these points is equal. The absorption driving force and the amount of mass transfer are directly governed by the compressor's discharge pressure, the inlet ammonia and solution concentrations. Similarly, in the desorber, desorption of refrigerant vapours from the strong solution by extracting heat from a heat source causes a decrease in solution concentration and an increase in desorber temperature. The path 3-4-5 is the weak solution path.

## 2.3 Different Types of Compression-Absorption Systems

Various types of compression-absorption systems have been explained in the following section.

### 2.3.1 Single stage compression-absorption system

This is the most common configuration of a compression-absorption system. It consists of a compressor incorporated in a solution circuit formed by an absorber, a desorber, a solution heat exchanger, a solution pump, and an expansion valve. A refrigerant-absorbent mixture circulates in the solution circuit, whose composition can be changed to achieve a wide range of capacities which is limited by the difference in the boiling points of the two constituents forming the mixture. A compressor is added to the solution circuit to raise the pressure of the refrigerant from the low desorber pressure to the high absorber pressure. The input of energy is in the form of work .

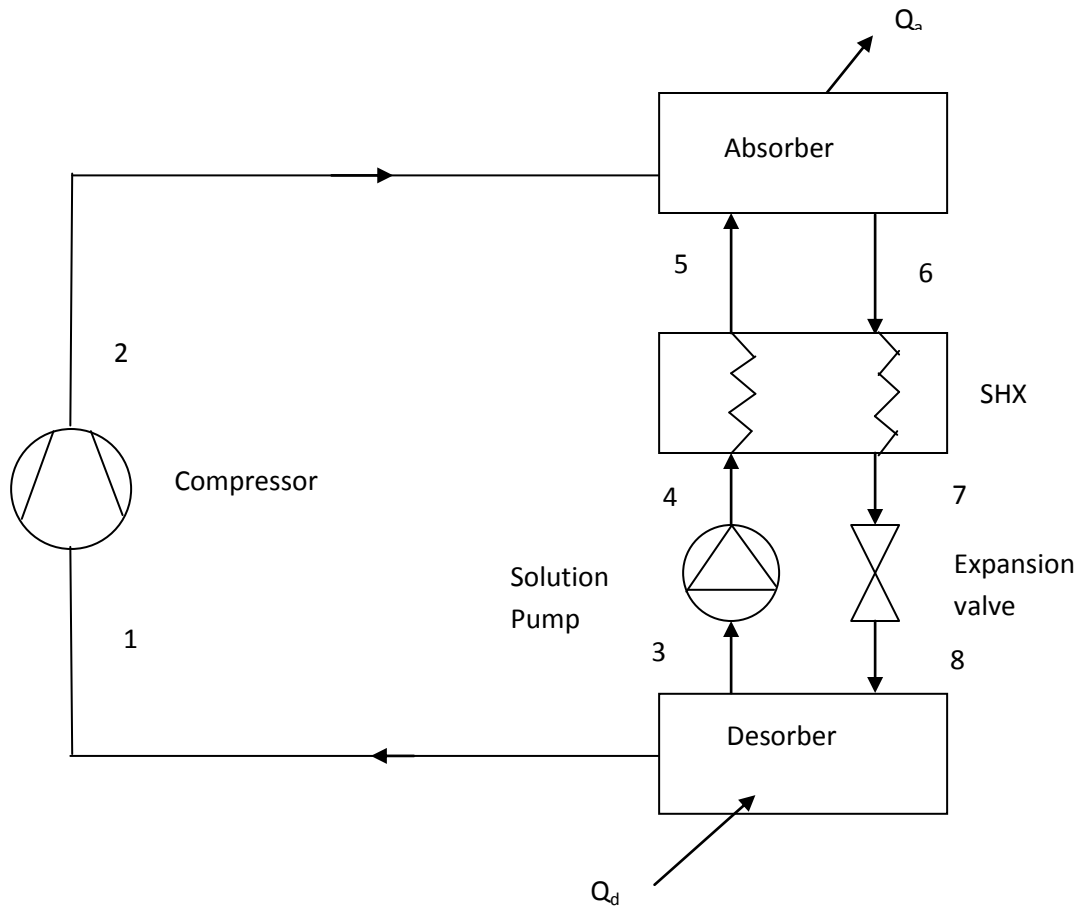


Fig.2.3.1 Schematic diagram of a single stage compression-absorption system

### 2.3.2 Two stage compression-absorption system

In this configuration, there are two loops, each consisting of an absorber, a desorber, a solution pump, a solution heat exchanger. Both the loops are served by the same compressor. The heat released by the absorber of first stage is fed as the heat input to the desorber of second stage. The desorber of the first stage extracts heat from an outside source and the absorber of the second stage rejects heat to an outside sink. This configuration is especially useful when large temperature lifts are required at very low pressure ratios.

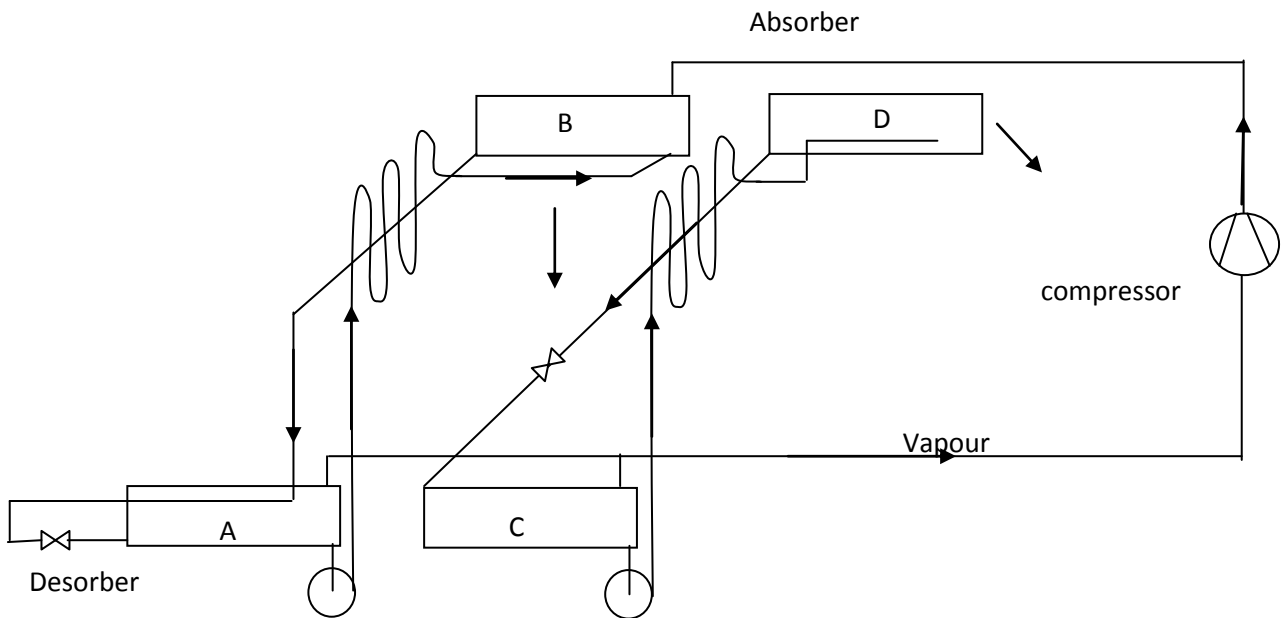


Fig.2.3.2 Schematic diagram of a two stage compression-absorption system

**2.3.3 Desorber-absorber heat exchange (DAHX) cycle-** In this configuration, there is an internal heat exchange between the main components of the system. It is a combination of the single-stage and two-stage cycle. Compared to the single-stage cycle, its main difference is the addition of an internal desorber-absorber heat exchanger instead of a solution heat exchanger. A large gliding temperature difference across the desorber and the absorber results in the temperature overlap between them, which means that the highest temperature in the desorber may be higher than the lowest temperature in the absorber [23].

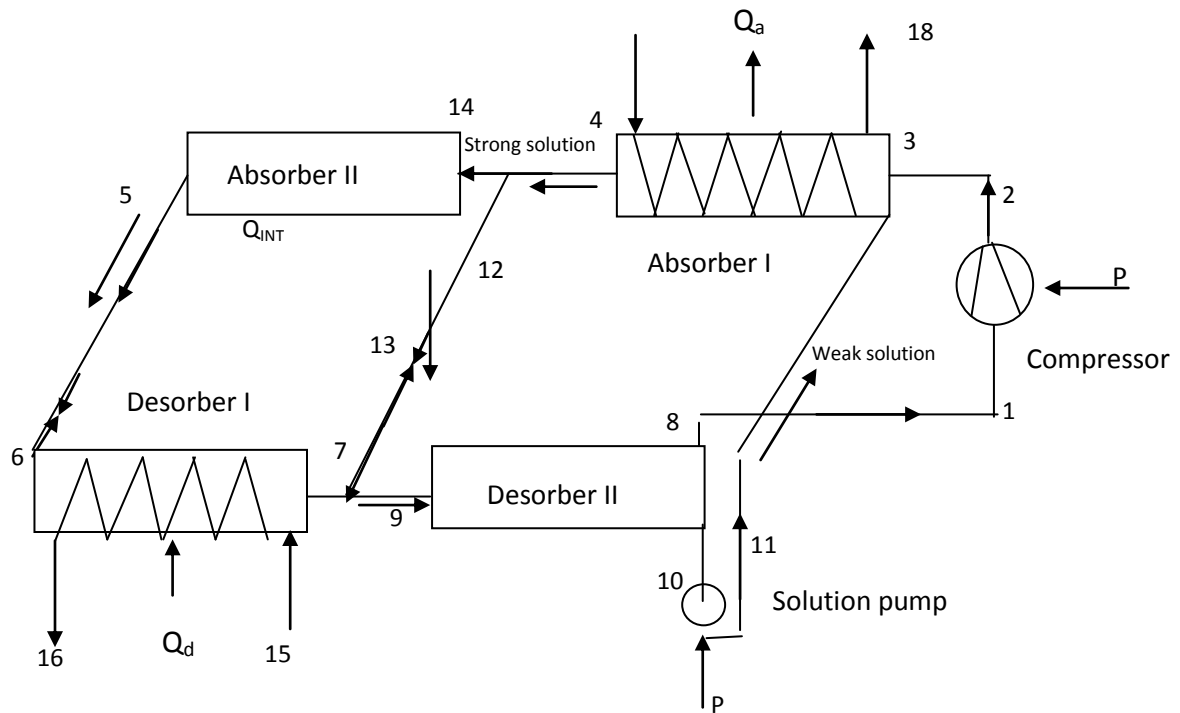


Fig.2.3.3 Schematic diagram of a DAHX compression-absorption system

## 2.4 Different Schedules of a Compression-Absorption System

Vapour compression can be introduced at different points of the sorption process cycle. Therefore, single, double, triple pressure stage types can be distinguished, depending upon the installation of a compressor between or in parallel to the absorber and the desorber [1]. These have been described in the following section.

### 2.4.1 Compression-absorption (CA) system with compressor between absorber and desorber

This is the most important system which is very simple and closely resembles a conventional compression system in which the evaporator and condenser are replaced by a desorber and a resorber respectively. A compressor is placed between absorber and desorber to raise the pressure of the refrigerant to a higher level. This results in an elementary sorption-compression heat pump with one pressure stage and two temperature levels. It is commonly termed as resorption compression system.

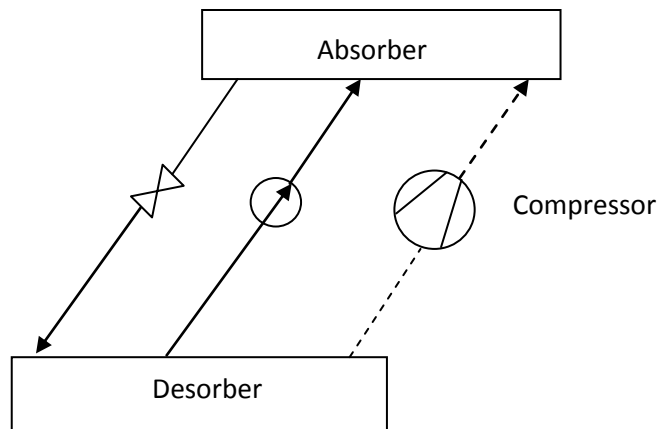


Fig. 2.4.1 compression-absorption system with compressor between absorber and desorber

**2.4.2 Compression-Absorption system with mechanical vapour compression between low and high pressure level of a sorption heat pump.**

In this layout, a compressor is placed in a parallel position to the desorber/absorber solution cycle of the elementary absorption heat pump. The compressor is either driven by an electrical or a combustion engine. The layout with an electrical engine can alternately be driven as a compression or an absorption heat pump depending upon the availability of the sources. The layout with a combustion engine can be used to improve COP if combustion exhaust gases are utilized as a high temperature heat source of the desorber.

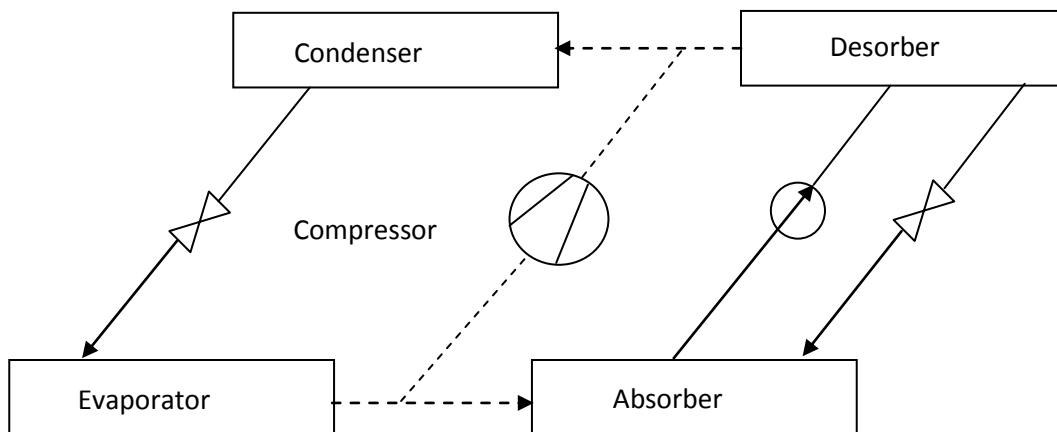


Fig. 2.4.2 compression-absorption system with mechanical vapour compression between low and high pressure level of a sorption heat pump.



**2.4.3 compression-absorption system with low pressure booster.** In this layout, a mechanical compressor is placed between the evaporator and absorber of the elementary absorption heat pump. The refrigerant vapour is first mechanically compressed by means of the compressor to a medium pressure level and then to a high pressure level by the solution pump. Hence, a two stage SC heat pump is obtained. This offers an advantage of utilizing low temperature heat sources. But it has the drawbacks of lower COP and a higher investment cost.

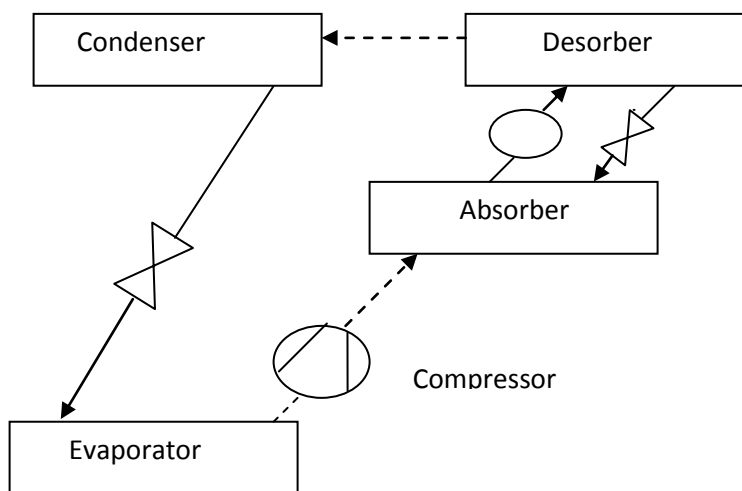


Fig.2.4.3 compression-absorption system with low pressure booster

**2.4.4 compression-absorption system with high pressure booster.**

In this layout a mechanical compressor is placed between the condenser and the desorber. The high pressure prevailing in the desorber is boosted to a higher level. Thus, the total temperature rise of the heat pumping process is increased. But the driving energy consumption is increased and there is high investment involved. By combining the low pressure and the high pressure booster types, a three-pressure stage compression-absorption system is obtained which was proposed for a hybrid solar air-conditioning system (Costello, 1976). Schematic diagram of this layout is shown in Fig. 2.9

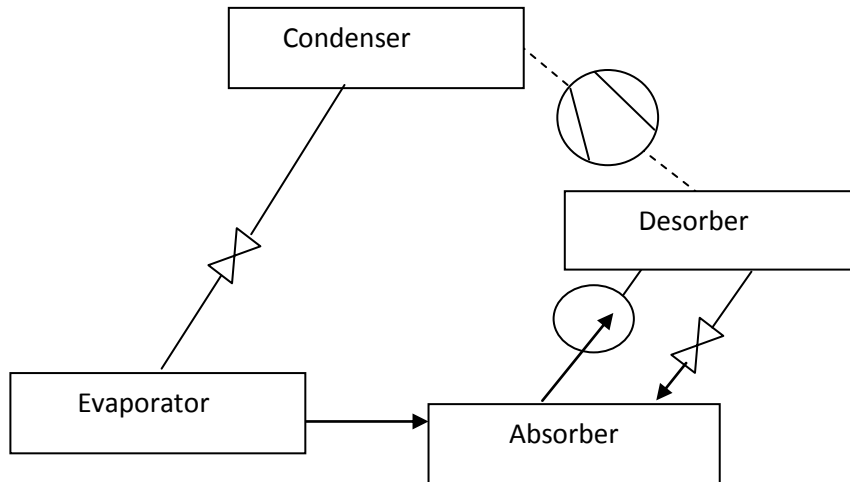


Fig. 2.4.4 Sorption-compression heat pump with high pressure booster

## 2.5 Theoretical Studies reported in the literature

Extensive studies have been carried out on the compression-absorption systems by various researchers regarding the first law analysis of the system as reported in the literature which are explained in the following section.

Morawetz [1] defined the elementary and improved sorption-compression heat pumps. He discussed the merits of the resorption-compression heat pumps. They reviewed the performance of an ammonia-water heat pump designed for the production of process vapour. The heat source was the expansion steam from waste water at a temperature of 95°C. They found the performance of this heat pump as impressive.

Minea and Chiriac [2] discussed the main thermodynamic and hydraulic parameters and gave design guidelines for a medium temperature, ammonia-water based compression-resorption heat recovery system for district domestic hot water production. They produced hot water at 55°C from cooling water at 36°C used as a waste heat source

Pourezza-Djourshari and Radermacher [3] presented the performance results of single and two stage vapour compression heat pumps with solution circuits both operating on R22-DEGDME mixture as the working fluid. The desorber temperatures considered were in the range -25°C to -20°C and 5 to 10°C and the absorber temperature was from 50°C to 60°C.

They found a significant increase in the coefficient of performance in both the cycles as compared to the R22. The COP of the two stage cycle was found to increase upto 50% at 45% lesser pressure ratio as compared to the conventional vapour compression system using pure R22 as the working fluid.

Arun et al [4] analysed a compression-absorption heat pump with a single stage solution circuit operating on HFC143a-Dimethylacetamide (DMAC) mixture. They studied the effects of suction and discharge pressures, generator and absorber temperatures on the performance parameters such as circulation ratio, coefficient of performance, and discharge temperature. They also compared the performance with that of the conventional HFC134a vapour compression heat pump and generated the operating domain diagram for various average solution concentrations. From the results obtained after their analysis, they found that at low pressure ratios and high temperature lifts, the compression-absorption heat pump gave better performance than compression system.

Brunnin et al [5] defined the model of a compression-absorption heat pump using ammonia-water mixtures. They also studied the working domains of a compression heat pump and a compression-absorption heat pump which were limited by the technical constraints of minimum coefficient of performance, minimum volumetric heating capacity, minimum low pressure and maximum high pressure. They found that the use of ammonia-water mixtures in a compression-absorption heat pump covered the whole working domain of high temperature heat pumps with performance comparable to that of compression heat pumps.

Ahlby et al [6] carried out the optimization study of the compression-absorption cycle working on ammonia-water mixture. They found the optimum operating point for the cycle corresponding to various external conditions. They also showed that the cycle performance can be improved by optimizing the temperature gradient in the absorber. They made comparison of the cycle with the vapour compression cycle working on pure R12 refrigerant and found a higher COP. COP of the CA cycle was found to be 9-21% higher than that for the R12 system.

George et al [7] carried out a thermodynamic study of a R22-DMF compression-absorption heat pump. They studied the effects of varying the temperatures in the absorber and the

desorber, pressure ratio of the compressor on the performance of the system. The absorber heat load was 1 kW, with the absorber temperature varying between 45°C to 85°C and the desorber temperature from 20°C to 40°C. They correlated the data resulted from the analysis and developed the expressions for the COP, CR, Concentration difference and the limiting temperature for the absorber.

Hulten and Berntsson [8] studied theoretically the performance improvement of an industrial single stage compression-absorption heat pump operating on an ammonia-water mixture. They found that higher COPs can be obtained if the pressure ratios are increased for such a heat pump. They suggested some design improvements for the heat pump which could raise its performance such as the use of longer falling film tubes in the absorber and the desorber increased the COP. They also compared the performance of the system with that of a two stage compression heat pump using isobutene as working fluid.

Hulten and Berntsson [9] studied the influence of some operating parameters such as the absorber glide, concentration change in the absorber, absorber and desorber falling film tube lengths, heat exchanger area distribution on the COP of a CAHP. They also compared an ammonia-water based CAHP with a CHP working on isobutane by considering the local heat transfer coefficients and the pressure drops. They observed that for large temperature glides (> 20 K), the CAHP gives 12% better performance than a CHP. They also found that for longer falling film tubes in the absorber and the desorber, the COP obtained was higher.

Boer et al [10] studied the performance of double effect absorption compression cycles using methanol-TEGDME and TFE-TEGDME as the working pairs. They found that performance of a double effect absorption cycle using these organic mixtures could be improved by introducing a compression stage between the evaporator and the absorber. They also observed that the cycle could work even if low grade heat was available as the heat source delivering higher COP.

Pratihari et al [11] performed thermodynamic modeling and feasibility analysis of a compression absorption refrigeration system working on ammonia-water mixture. He studied the effects of various operating parameters like the absorber and desorber temperatures, compression ratio and heat exchanger effectiveness on the coefficient of

performance. He obtained a COP of 5.39 at an absorber pressure of 20 bar, desorber temperature of 40°C, compression ratio of 4 and heat exchanger effectiveness of 0.7.

Ferreira et al [12] investigated the performance of a twin screw compressor operating under two phase compression for an ammonia-water CAHP cycle both theoretically and experimentally. They have tried to increase the isentropic efficiency of the compressor that makes wet compression-absorption heat pumps a competitive technical option.

Bourouis et al [13] studied the thermodynamic performance of a single stage absorption/compression heat pump using the ternary working fluid TFE-H<sub>2</sub>O-TEGDME for upgrading the waste heat. They developed a simulation program based on mass and energy balance of all the components of the cycle. It was concluded that operation of the cycle with ternary mixture was more advantageous than the binary mixture TFE-TEGDME.

Tarique and Siddiqui [14] performed a performance study and economic analysis of the combined absorption/compression cycle using NH<sub>3</sub>-NaSCN solution and compared it with the performance of a vapour compression cycle operating on pure ammonia. The result obtained was better performance at lower pressure ratios and high absorber temperature. They found that the performance of NH<sub>3</sub>-NaSCN in the combined cycle for fixed values of the heating temperature are nearly 30-60% higher than that in the pure ammonia compression cycle.

Kilic and Kaynakli [15] analyzed the single stage water-lithium bromide absorption refrigeration system using the first and the second laws of thermodynamics. They introduced a mathematical model based on the exergy method to evaluate the system performance, exergy loss of each component and total exergy loss of all the system components. Various performance parameters like coefficient of performance (COP), circulation ratio (CR), exergetic efficiency and efficiency ratio were calculated from the thermodynamic properties of the working fluids at various operating conditions. It was shown that the performance of the absorption refrigeration system increased with increasing generator and evaporator temperatures, but decreased with increasing condenser and absorber temperatures. Exergy losses in the expansion valves, pump and heat exchangers were small compared to other components.

Talbi and Agnew [16] carried out exergy analysis on a single effect absorption refrigeration cycle with lithium bromide-water as the working fluid pair. Numerical results for the cycle were tabulated. A design procedure was applied to a lithium bromide absorption cycle and an optimization procedure that consists of determining the enthalpy, entropy, temperature, mass flow rate, heat rate in each component and coefficient of performance was calculated.

Arora and Kaushik [17] presented a detailed exergy analysis of an actual vapour compression refrigeration (VCR) cycle. They developed a computational model for computing coefficient of performance (COP), exergy destruction, exergetic efficiency and efficiency defects for R502, R404A and R507A. They investigated the system for evaporator and condenser temperatures in the range of  $-50^{\circ}\text{C}$  to  $0^{\circ}\text{C}$  and  $40^{\circ}\text{C}$  to  $55^{\circ}\text{C}$  respectively. R507 was found to be a better substitute to R502A than R404A. The condenser was found to be the worst component from the point of view of exergy destruction followed by compressor, throttle valve and evaporator respectively. They also studied the effect of dead state temperature on the exergetic efficiency and the exergy destruction ratio and found that an increase in dead state temperature had a positive effect on both of them. They also considered the pressure drops in condenser and evaporator to study their effects on the exergetic efficiency and the exergy destruction ratio.

## **2.6 Conclusion**

The above literature review reveals that this technology is still at its developmental stage. Although many works have been conducted to analyze the performance of a compression-absorption system, few attempts have been made to modify it. There has been enormous work done on the first law analysis of the system but very little work regarding the second law analysis has been reported in the literature.

## THERMODYNAMIC ANALYSIS OF A COMPRESSION- ABSORPTION SYSTEM

A single stage compression-absorption heat pump under study has been described in this section to know about the various components comprising the system and the flow of the fluid across them.

### 3.1 Description of a Single Stage Compression-Absorption Heat Pump

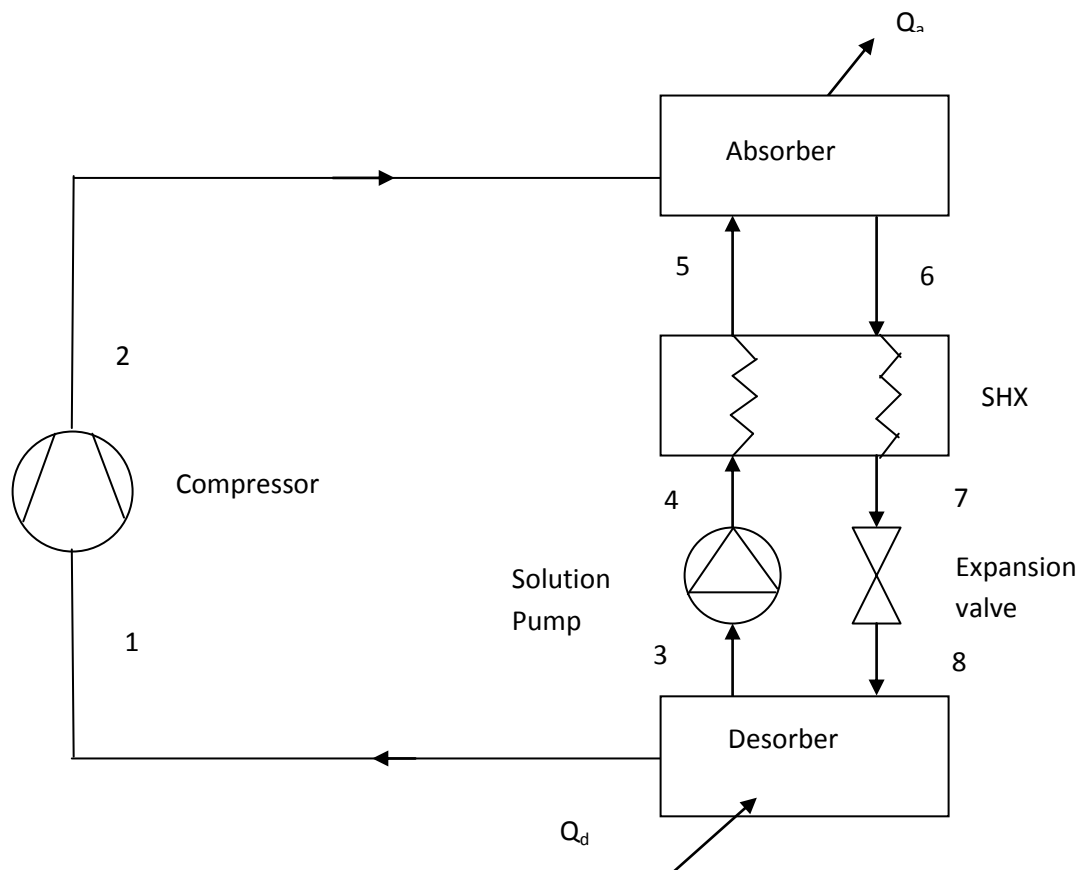


Fig. 3.1 Schematic diagram of a compression-absorption system

The compression absorption heat pump cycle combines two well known heat pump concepts viz. the compression heat pump and the absorption heat pump. To create the hybrid cycle, the condenser and the evaporator in a conventional vapour compression heat pump are

replaced by an absorber and a desorber. The various components forming a compression-absorption system are an absorber, a desorber, a solution heat exchanger, solution pump, expansion valve which form the solution circuit, where the weak and the strong solution of the ammonia-water mixture circulates. A compressor is connected to the solution circuit part of the cycle to raise the pressure of the ammonia vapours from the desorber pressure to the absorber pressure.

In a compression-absorption cycle, the ammonia vapours enters the compressor at state point 1, where they are compressed to the higher absorber pressure requiring the compressor work. At the state point 2, the compressed ammonia vapours leaves the compressor in a superheated state. Both the temperature and pressure are increased with the concentration remaining constant. The high pressure ammonia vapours from the compressor enter the absorber at point 2. The weak solution of ammonia and water from the solution heat exchanger enters the absorber at point 5. The absorption of ammonia vapours into the weak solution leads to the formation of strong solution which has the higher concentration of  $\text{NH}_3$ . This process is accompanied by a rejection of heat. The absorption process takes place over a range of temperatures. In the absorber, as the concentration of the ammonia increases the temperature decreases at a constant pressure. When the concentration reaches a maximum value, the strong solution leaving the absorber at state point 6 becomes saturated. The pressure of the weak solution leaving the desorber at state point 3 is raised to the absorber pressure, that is the higher pressure level of the cycle, by means of a solution pump. A regenerative solution heat exchanger is placed to transfer heat from the hot, strong solution leaving the absorber to the cold, weak solution entering the absorber.

### **3.2 Assumptions Taken into Consideration for the Analysis**

The thermodynamic analysis of the compression-absorption heat pump is carried out by making the following assumptions:

1. System is at steady state condition.
2. The absorber and the desorber outlets are assumed to be at saturated states.
3. Isenthalpic expansion occurs across the expansion valve.



4. The undesirable heat losses and pressure drops in various components and pipe lines, are neglected.
5. Pump efficiency is assumed to be 70%.

### 3.3 p-T-x Relations for the Ammonia-Water Mixture

Prior to defining the mass, material and energy balance equations for all the components making up the system, the relation between pressure, temperature and concentration for a binary mixture like ammonia-water must be known. These relations have been presented under this section.

Concentrations of strong solution leaving the absorber and the weak solution leaving the desorber can be stated by the following P-t-x relation: (Borde et al., 1991)

$$x_{ss} = f(p_d, t_a) \quad (3.1)$$

$$x_{ws} = f(p_s, t_d) \quad (3.2)$$

where,  $p_d$  = Discharge pressure.

$p_s$  = suction pressure.

$x_{ss}$  = concentration of strong ammonia-water solution.

$x_{ws}$  = concentration of weak ammonia-water solution.

$t_a$  = absorber temperature.

$t_d$  = desorber temperature.

Specific volume and the enthalpy of the ammonia vapour entering the compressor are defined according to the following relation:

$$v_1 = f(p_s, t_d) \quad (3.3)$$

$$h_1 = f(p_s, t_d) \quad (3.4)$$

where,  $v_1$  = specific volume of the refrigerant vapour at the inlet of the compressor.

$h_1$  = enthalpy of the ammonia vapour at the compressor inlet.

The enthalpy of the saturated solution leaving the absorber and desorber are defined as per the following relation:

$$h_6 = f(t_d, x_{ss}) \quad (3.5)$$

$$h_3 = f(t_d, x_{ws}) \quad (3.6)$$

where, subscripts, '3' and '6' represents the exit states of desorber and the absorber respectively.

### 3.4 First Law Analysis

For the thermodynamic analysis of the compression-absorption system the principles of first and second laws of thermodynamics are applied to each component of the system. Each component can be treated as a control volume with inlet and outlet streams, heat transfer and work interactions. The first law analysis comprises of the mass, material and energy balance applied to all the components forming the whole system. The governing equations of mass, material and energy balance for a steady state and steady flow system are:

$$\Sigma m_i - \Sigma m_o = 0 \quad (3.7)$$

where,  $m$  = mass flow rate.

Subscripts 'i' and 'o' represents inlet and outlet streams respectively.

According to the mass conservation principle, the sum total of all the masses entering into the system must be equal to the sum of all the masses leaving that system. In other words, there is no accumulation of mass within a system.

The material balance in the system can be expressed as:

$$\Sigma (mx)_i - \Sigma (mx)_o = 0 \quad (3.8)$$

where,  $x$  is mass concentration of  $\text{NH}_3$  in the ammonia-water solution.

The first law of thermodynamics yields the energy balance of each component of a system as follows:

$$\Sigma (mh)_i - \Sigma (mh)_o + [\Sigma Q_i - \Sigma Q_o] + W = 0 \quad (3.9)$$

where,  $Q$  = Heat flow rate in kW.

$h$  = specific enthalpy in kJ/kg.

$W$  = Work interaction in kW.

On applying the first law principles on the compression-absorption heat pump considered in the present study, yield the following set of equations.

### 3.4.1 Governing equations based on first law analysis

For each component of system, the mass, material and energy balance equations have been written which are presented in this section.

#### ***Absorber:***

The mass balance equation can be expressed as:

$$m_2 + m_5 = m_6 \quad (3.10)$$

The component balance equation is given by:

$$m_2 x_2 + m_5 x_5 = m_6 x_6 \quad (3.11)$$

The energy balance equation is:

$$m_2 h_2 + m_5 h_5 = m_6 h_6 + Q_a \quad (3.12)$$

where,  $m$  = mass flow rate in kg/s.

$x$  = ammonia concentration in ammonia-water solution.

$h$  = enthalpy in kJ/kg.

$Q_a$  = Heat rejected by the absorber in kW.

subscripts '2' and '5' refer to the inlet streams. '6' represents the stream leaving the absorber. By solving these three equations, the mass flow rate of the strong solution coming out of the absorber  $m_6$ , mass flow rate of the weak solution entering the absorber  $m_5$ , and that of the compressed vapour coming out of the compressor  $m_2$  are obtained. The mass flow rate of the weak solution entering the absorber is given by:

$$m_5 = m_2 \frac{x_2 - x_6}{x_6 - x_5} \quad (3.13)$$

The mass flow rate of the strong solution coming out of the absorber can be expressed as:

$$m_6 = \frac{Q_a}{h_2 \frac{x_6 - x_5}{1 - x_5} + h_5 \frac{1 - x_6}{1 - x_5} - h_6} \quad (3.14)$$

**Desorber:**

The mass balance equation for the desorber is :

$$m_1 + m_3 = m_8 \quad (3.15)$$

The component balance equation for the desorber is given as:

$$m_1 x_1 + m_3 x_3 = m_8 x_8 \quad (3.16)$$

The energy balance equation is :

$$m_1 h_1 + m_3 h_3 = m_8 h_8 + Q_d \quad (3.17)$$

where,  $Q_d$  = Heat absorbed by the desorber when the refrigerant vapours are separated from the strong solution leaving the weak solution to enter the solution pump. subscripts '8' refers

to the entering strong solution stream into the desorber. '1' and '3' refer to the refrigerant vapours leaving the desorber and the weak ammonia-water solution leaving the desorber respectively.

***Solution heat exchanger:***

$$m_6 h_6 + m_4 h_4 = m_5 h_5 + m_7 h_7 \quad (3.18)$$

Effeciveness of the solution heat exchanger( $\varepsilon$ ) has been defined by the Eqn. (3.19).

$$\varepsilon = \frac{h_5 - h_4}{h_6 - h_4} \quad (3.19)$$

where,  $h_4$ = enthalpy of the strong solution at the temperature  $t_4$ , which is the minimum possible temperature at point 7.

***Compressor:***

The compressor work can be calculated as:

$$W_c = m_2 \frac{h_2 - h_1}{\eta_c} \quad (3.20)$$

where,  $W_c$  = work input to the compressor in kW.

$\eta_c$  = isentropic efficiency of the compressor.

***Expansion valve:***

The isenthalpic expansion process in the expansion valve can be stated as:

$$h_7 = h_8 \quad (3.21)$$

***Solution pump:***

The pump work is given by:

$$W_p = m_3 v_3 \frac{p_4 - p_3}{\eta_p} \quad (3.22)$$

where,  $W_p$  = Pump work in kW.

$\eta_p$  = Pump efficiency.

Some important parameters can be defined as:

The pressures at points 2,4,5,6,7 is the same and is the higher pressure in the system.

$$p_2 = p_4 = p_5 = p_6 = p_7 = P_{high} \quad (3.23)$$

The pressures at points 1,3,8 is the same and is the lower pressure of the system.

$$p_1 = p_3 = p_8 = P_{low} \quad (3.24)$$

The mass flow rate and the concentration for the weak solution path i.e., 3-4-5 is :

$$m_3 = m_4 = m_5 = m_{ws} \quad (3.25)$$

where,  $m_{ws}$  = mass flow rate of the weak solution.

$$x_3 = x_4 = x_5 = x_{ws} \quad (3.26)$$

$x_{ws}$  = concentration of the weak solution.

Similarly, the mass flow rate and the concentration for the strong solution path i.e., 6-7-8 is

$$m_6 = m_7 = m_8 = m_{ss} \quad (3.27)$$

$$x_6 = x_7 = x_8 = x_{ss} \quad (3.28)$$

where,  $m_{ss}$  = mass flow rate of the strong solution.

$x_{ss}$  = concentration of the strong solution.

### 3.4.2 Terminology and performance parameters related to the first law analysis

The performance parameters that can be used to evaluate the performance of a compression-absorption system can be explained as follows:

- **Coefficient of performance (COP):** It is defined as the ratio of the output to that of the input.

$$\text{COP} = \frac{Q_a}{W_c + W_p} \quad (3.29)$$

- **Circulation ratio (CR):** It is the ratio of the mass flow rate of the strong solution to that of ammonia vapours.

$$\text{CR} = \frac{m_6}{m_1} = \frac{1 - x_3}{x_6 - x_3} \quad (3.30)$$

- **Absorber glide ( $T_{GA}$ ):** The change in the temperature of the working fluid during absorption in the absorber.

$$T_{GA} = T_5 - T_6 \quad (3.31)$$

where,  $T_5$  is the equilibrium temperature corresponding to the absorber pressure and weak solution concentration.

- **Desorber glide ( $T_{GD}$ ):** The temperature change of the working fluid during desorption in the desorber.

$$T_{GD} = T_3 - T_8 \quad (3.32)$$

where,  $T_3$  is the equilibrium temperature corresponding to the desorber pressure and strong solution concentration. Thus the temperature glides calculated are the maximum possible values for a given pressure and concentration.

### 3.5 Second Law Analysis

The second law analysis can be used to calculate the system performance based on exergy. Exergy is defined as the maximum useful work that could be obtained from a system at a given state with respect to a reference environment (dead state). In a process or a system the total amount of exergy is not conserved but is destroyed due to internal irreversibilities. Exergy analysis is the combination of the first and second laws of thermodynamics. The exergy of a fluid stream can be defined as:

$$\Psi = (h - h_0) - T_0(s - s_0) \quad (3.33)$$

where ,  $\psi$  = specific exergy of the fluid in kJ/kg at temperature T.

$h$  = specific enthalpy in kJ/kg.

$s$  = specific entropy in kJ/kgK.

$0$  = reference or dead state.

In a thermodynamic system, exergy can be transferred to or from a system in three forms: heat, work and mass flow, which are recognized at the system boundaries. The exergy transfer by heat can be expressed as:

$$\psi_h = 1 - \frac{T_0}{T} \cdot Q \quad (3.34)$$

where,  $T_0$  = temperature of the environment in K.

$T$  = temperature of the heat source in K.

In case of the mechanical work interaction across the system boundaries, the exergy transfer is equal to the mechanical work itself. For the mass flow across the system, the exergy transfer can be expressed as:

$$\Psi_m = m\Psi \quad (3.35)$$

where,  $m$  = mass flow rate crossing the system boundaries in kg/s.

$\Psi$  = specific exergy in kJ/kg.

For a steady flow process, the exergy balance equation can be written as:

$$E_{in} = E_{destroyed} + E_{out} \quad (3.36)$$

where,  $E$  = exergy in kW.

Exergy destruction in a process is the product of entropy generated and the reference environment temperature  $T_0$ .

$$E_{destroyed} = T_0(S_{generation}) \quad (3.37)$$



The exergy loss in each component is calculated by:

$$\Delta\psi = \Sigma m_i \Psi_i - \Sigma m_o \Psi_o - [\Sigma Q(1 - \frac{T_0}{T})_i - \Sigma Q(1 - \frac{T_0}{T})_o] + \Sigma W \quad (3.38)$$

where,  $\Delta\Psi$  is the lost exergy or irreversibility that occurred in the process.

The first two terms of the right hand side of Eq. (3.37) are the exergy of the inlet and outlet streams of the control volume. The third and fourth terms are the exergy associated with the heat transferred from the source maintained at a temperature  $T$ . The last term is the exergy of mechanical work added to the control volume.

The second law efficiency of a compression-absorption system is measured by the exergetic efficiency,  $E$ , which is defined as the ratio of the useful exergy gained from a system to that supplied to the system.

On applying the second law principles on the compression-absorption heat pump considered in the present study, yield the following set of equations.

### 3.5.1 Governing equations based on second law analysis

The set of equations that are used to analyse a compression-absorption heat pump based on second law are discussed in this section.

#### **Absorber:**

The exergy loss in the absorber can be expressed as:

$$\Delta\Psi_a = m_2 \Psi_2 + m_5 \Psi_5 - m_6 \Psi_6 + Q_a (1 - \frac{T_0}{T_6}) \quad (3.39)$$

$$\text{where, } \Psi_2 = (h_2 - h_0) - T_0 (s_2 - s_0) \quad (3.40)$$

$$\Psi_5 = (h_5 - h_0) - T_0 (s_5 - s_0) \quad (3.41)$$

$$\Psi_6 = (h_6 - h_0) - T_0 (s_6 - s_0) \quad (3.42)$$

$T_0$  = reference temperature of the environment.

$Q_a$  = heat rejected by the absorber in kW.

**Compressor:**

The exergy loss in the compressor is defined according to the following relation:

$$\Delta\Psi_c = m_1(\Psi_1 - \Psi_2) + W_c \quad (3.43)$$

$\Psi_1, \Psi_2$  = specific exergies at inlet and outlet of the compressor respectively.

**Desorber:**

The exergy loss in the desorber can be calculated using Eqn. (3.44).

$$\Delta\Psi_d = m_8\Psi_8 - m_3\Psi_3 - m_1\Psi_1 + Q_d \left(1 - \frac{T_0}{T_3}\right) \quad (3.44)$$

where,  $Q_d$  = heat input to the desorber in kW.

**Solution heat exchanger:**

The exergy loss in the solution heat exchanger is only due to the mass flow as there is no heat or work interaction with the surroundings. It is given as:

$$\Delta\Psi_{shx} = m_4\Psi_4 + m_6\Psi_6 - m_5\Psi_5 - m_7\Psi_7 \quad (3.45)$$

**Solution pump:**

The exergy loss in the solution pump due to mass flow and work interaction can be expressed as:

$$\Delta\Psi_p = m_3\Psi_3 - m_4\Psi_4 + W_p \quad (3.46)$$

**Expansion valve:**

The exergy loss in the expansion valve is :

$$\Delta\Psi_{ev} = m_7\Psi_7 - m_8\Psi_8 \quad (3.47)$$

After defining the expressions for exergy loss in all the components of the system, the total exergy loss for the whole system can be computed as:

$$\Delta\Psi_{tot} = \Delta\Psi_a + \Delta\Psi_c + \Delta\Psi_d + \Delta\Psi_{shx} + \Delta\Psi_p + \Delta\Psi_{ev} \quad (3.48)$$

### 3.5.2 Terminology and performance parameters related to second law analysis.

The important terms that are used to evaluate the performance of the compression-absorption heat pump based on second law analysis are described below:

**Exergetic efficiency ( $\eta_{ex}$ ):** It is defined as the ratio of the useful exergy gained from a system to that supplied to the system.

It is the ratio between exergy rate of product and fuel.

$$\eta_{ex} = \frac{Q_a \left(1 - \frac{T_3}{T_6}\right)}{W_c + W_p} \quad (3.49)$$

**Exergy destruction ratio (EDR):** It compares the exergy destruction in a component with the total exergy destruction of the whole system. It is defined as the ratio of the individual exergy loss of a component to that of the total exergy loss of the whole system.

$$\text{EDR} = \frac{\Delta\Psi_k}{\Delta\Psi_t} \quad (3.50)$$

where, k refers to individual component of the system.

**Efficiency defect ( $\delta_k$ ):** Efficiency defect is defined as the ratio between the exergy destroyed in each component and the exergy flow required to sustain the process (Kotas, 1985) and can be given by the following relation:

$$\delta_k = \frac{\Delta\Psi_k}{W_c + W_p} \quad (3.51)$$

### PROBLEM FORMULATION AND SOLUTION METHODOLOGY

#### 4.1 Problem Formulation

Analysis of an ammonia-water compression-absorption heat pump of 100 kW heating capacity has been carried out in this work. The input parameters taken are absorber pressure = 20 bar, desorber pressure = 4 bar, absorber load = 100 kW, absorber temperature = 50-80°C, desorber temperature = 30-40°C. By carrying out the thermodynamic analysis of the system for the conditions stated above the values of temperature, pressure and concentration at various state points of the cycle have been obtained. The computer program developed in EES calculates the performance parameters of the system such as coefficient of performance, circulation ratio, solution heat exchanger effectiveness, compressor work, pump work from the first law analysis and exergetic efficiency, exergy destruction ratio from the second law analysis.

#### 4.2 Solution Methodology In Engineering Equation Solver (EES)

EES is a software package developed by Dr. Sanford Klein of the University of Wisconsin. EES incorporates the programming structures of C and FORTRAN with a built-in iterator, thermodynamic and transport property relations, graphical capabilities, numerical integration, and many other useful mathematical functions. By grouping equations that are to be solved simultaneously, EES is able to function at a high rate of computational speed. Ammonia-water mixture properties are calculated in EES using the correlation developed by Ibrahim and Klein (1993). There are two major differences between EES and existing numerical equations solving programs. First, EES automatically identifies and groups equations that must be solved simultaneously. This feature simplifies the process for the user and ensures that the solver will always operate at optimum efficiency. Second, EES provides many built-in mathematical and thermophysical property functions useful for engineering calculations. The basic function provided by Engineering Equation Solver (EES) is the numerical solution of non-linear algebraic and differential equations, EES provides built-in thermodynamic and transport property functions for many fluids including water, dry and

moist air. Included in the property database are thermodynamic properties for H<sub>2</sub>O-LiBr and NH<sub>3</sub>-H<sub>2</sub>O mixtures. Any information between quotation marks[""] or braces [{}] is an optional comment. Variable names must start with a letter. The NH<sub>3</sub>-H<sub>2</sub>O properties are not integral part of the EES program but are instead provided by external routines. The NH<sub>3</sub>-H<sub>2</sub>O properties for each state are determined through a call to the external NH<sub>3</sub>-H<sub>2</sub>O program. Three independent properties are needed to fix each state.

The calling format for the ammonia-water procedure is

**CALL NH3H2O (Code, In1,In2,In3:T,P,x,h,s,u,v,Q)**

The four parameters to the left of the colon are inputs. The parameters to the right of the colon are outputs. The NH3H2O routine operates in SI units with T=[K], P= [bar], x= [ammonia mass fraction], h = [KJ/Kg], s=[KJ/KgK], u = [KJ/Kg], v= [m<sup>3</sup>/Kg] and Q= [vapor mass fraction].

For saturated states :  $0 \leq Q \leq 1$

Saturated liquid: Q=0

Saturated vapour: Q=1

Subcooled states: Q= -0.01

Superheated states: Q= 1.01

A code containing a good library of working fluid properties suitable for heat pumps is the Engineering Equations Solver (EES) [24]. Here the user must write the equations governing the cycle and make sure the set is well-defined. In the case of a non-linear set of equations, the user must check the results to make sure that the mathematical solution is also a physical one. In one form or another, the user has to do a fair amount of programming to lead the simulator toward convergence to the correct solution.

### 4.3 Computer Program and Its Output

The computer program for the investigation of the first and second law analysis of a compression-absorption heat pump developed in EES has been given here along with its output. The initial conditions read into the program include the ambient conditions, heat exchanger effectiveness, absorber and desorber pressures and temperatures. With the given parameters, the program calculates at all points of the cycle the values of temperature, enthalpy, entropy, mass flow rate, concentration and exergy of the mixture. The COP and exergy efficiency are also estimated.

### 4.4 Performance Calculations

The performance of the system has been calculated by using the above said computer program. The results of one sample calculation have been shown in the Appendix.1.

#### "! Compression-Absorption cycle calculations"

```
FUNCTION tk(T)                                {converts from C to K}
tk:=ConvertTemp('C', 'K', T)                "It is easier to type tk(T) than ConvertTemp('C','K',T)"
END
```

#### "!absorber"

```
P_high= 20 [bar]
P_low= 4 [bar]
Q_abs=100
CALL NH3H2O(234, P_high, x_3,h_5e: T_5, P_5, x_5, h_5, s_5, u_5, v_5, Qu5)
CALL NH3H2O(235, P_high, x_1,s_1: T_2, P_2, x_2, h_2, s_2, u_2, v_2, Qu2)
CALL NH3H2O(128,tk(T[6]), P_high, 0: T_6, P_6, x_6, h_6, s_6, u_6, v_6, Qu6)
m_2+m_5=m_6                                {mass balance}
m_2*x_2+m_5*x_5=m_6*x_6                    {ammonia balance}
h_2n*m_2+h_5*m_5-h_6*m_6-Q_abs=0           {energy balance}
```

### "!Generator Heat Exchanger"

epsilon=0.7 *{effectiveness of heat exchanger}*  
m\_5\*(h\_5e-h\_4)=m\_6\*(h\_6-h\_e)  
CALL NH3H2O(234,P\_high,x\_6,h\_e: T\_7, P\_7, x\_7, h\_7, s\_7, u\_7, v\_7, Qu7)  
epsilon=(h\_5e-h\_4)/(h\_6-h\_4)

### "!compressor"

CALL NH3H2O(128,T\_3, P\_low,1: T\_1, P\_1, x\_1, h\_1, s\_1, u\_1, v\_1, Qu1)  
CALL NH3H2O(234, P\_high, x\_1,h\_2n: T\_2n1, P\_2n1, x\_2n1, h\_2n1, s\_2n1, u\_2n1, v\_2n1, Qu2n1)  
W\_c=m\_1\*(h\_2n-h\_1)  
h\_2n=h\_1+(h\_2-h\_1)/eff\_c  
eff\_c=0.70 *{compressor efficiency}*

### "!throttle valve"

CALL NH3H2O(234, P\_low, x\_7,h\_7: T\_8, P\_8, x\_8, h\_8, s\_8, u\_8,v\_8,Qu8)

### "!solution pump"

eff\_pump=0.70 *{pump efficiency}*  
W\_p=m\_3\*v\_3\*(P\_high-P\_low)/eff\_pump  
h\_4=h\_3+W\_p/m\_3  
CALL NH3H2O(234, P\_high,x\_3,h\_4: T\_4, P\_4, x\_4, h\_4\_1, s\_4, u\_4, v\_4, Qu4)

### "!desorber"

CALL NH3H2O(128,tk(30[C]), P\_low,0: T\_3, P\_3, x\_3, h\_3, s\_3, u\_3, v\_3, Qu3)  
m\_1=m\_2  
m\_3=m\_5  
m\_8=m\_6  
m\_1\*h\_1+m\_3\*h\_3=m\_8\*h\_8+Q\_des *{energy balance}*

### "!overall"

$$\text{COP}=\text{Q\_abs}/(\text{W\_c}+\text{W\_p})$$

$$\text{Q\_check}=\text{Q\_abs}-\text{Q\_des}-\text{W\_c}-\text{W\_p}$$

$$\text{CR}=\text{m}_6/\text{m}_1$$

### **"!exergy analysis"**

$$\text{T}_0=\text{TK}(25[\text{C}]) \quad \{ambient\ temperature\}$$

### **"compressor"**

$$\text{DELTA\_PHI\_comp1}=\text{m}_1*(\text{h}_1-\text{h}_2)-\text{T}_0*(\text{s}_1*\text{m}_1-\text{s}_2*\text{m}_1) +\text{Wc}$$

### **"absorber"**

$$\text{DELTA\_PHI\_abs}=(\text{m}_1*\text{h}_2+\text{m}_3*\text{h}_5-\text{m}_6*\text{h}_6)-\text{T}_0*(\text{m}_1*\text{s}_2+\text{m}_3*\text{s}_5-\text{m}_6*\text{s}_6)-\text{Q\_abs}*(1-\text{T}_0/\text{T}_6)$$

### **"desorber"**

$$\text{DELTA\_PHI\_des}=(\text{m}_6*\text{h}_8-\text{m}_1*\text{h}_1-\text{m}_3*\text{h}_3)-\text{T}_0*(\text{m}_6*\text{s}_8-\text{m}_1*\text{s}_1-\text{m}_3*\text{s}_3)+\text{Q\_des}*(1-\text{T}_0/\text{T}_3)$$

### **"expansion valve"**

$$\text{DELTA\_PHI\_ev}=\text{m}_6*(\text{h}_7-\text{h}_8)-\text{T}_0*(\text{m}_6*\text{s}_7-\text{m}_6*\text{s}_8)$$

### **"solution pump"**

$$\text{DELTA\_PHI\_pump1}=\text{W\_p}-\text{m}_3*(\text{h}_3-\text{h}_4)+\text{T}_0*(\text{m}_3*\text{s}_3-\text{m}_3*\text{s}_4)$$

### **"solution heat exchanger"**

$$\text{DELTA\_PHI\_shx}=\text{m}_6*(\text{h}_6-\text{h}_7)-\text{T}_0*(\text{m}_6*\text{s}_6-\text{m}_6*\text{s}_7)+\text{m}_3*(\text{h}_4-\text{h}_5)-\text{T}_0*(\text{m}_3*\text{s}_4-\text{m}_3*\text{s}_5)$$

### **"overall exergy destruction of the system"**

$$\text{DELTA\_PHI\_total}=\text{DELTA\_PHI\_comp}+\text{DELTA\_PHI\_abs}+\text{DELTA\_PHI\_des}+\text{DELTA\_PHI\_ev}+\text{DELTA\_PHI\_pump}+\text{DELTA\_PHI\_shx}$$



**“Exergy destruction ratio of the components”**

$$\text{EDR}_c = (\text{DELTA\_PHI\_comp} / \text{DELTA\_PHI\_total}) * 100$$

$$\text{EDR}_a = (\text{DELTA\_PHI\_abs} / \text{DELTA\_PHI\_total}) * 100$$

$$\text{EDR}_{ev} = (\text{DELTA\_PHI}_{ev} / \text{DELTA\_PHI\_total}) * 100$$

$$\text{EDR}_p = (\text{DELTA\_PHI\_pump} / \text{DELTA\_PHI\_total}) * 100$$

$$\text{EDR}_{shx} = (\text{DELTA\_PHI}_{shx} / \text{DELTA\_PHI\_total}) * 100$$

**“exergetic efficiency”**

$$\text{Eff}_{exer} = Q_{abs} * (1 - T_3 / T_6) / (W_c + W_p)$$

### RESULTS AND DISCUSSION

In this study, the first and second law thermodynamic analysis of a single-stage compression-absorption system with ammonia-water as working fluid pair is performed. Thermodynamic properties of each point (the inlet and outlet of each component) in the cycle are calculated using related equations of state. Heat transfer rate of each component in the cycle and some performance parameters (circulation ratio CR, coefficient of performance COP) are calculated from the first law analysis. From the second law analysis, the exergy destruction of each component and the total exergy destruction of all the system components are obtained. Variation of the performance and exergy destruction of the system are examined at various operating conditions. Simulation results are presented in tabular and graphical form. The results of the first and second law analysis of the system, done with the help of a program developed in Engineering Equation Solver software have been presented in this chapter. The computer program developed within this project calculates the performance for the compression-absorption heat pump. The performance of a system is strongly dependent on how the operating conditions are chosen.

#### 5.1 Operating Conditions

The operating conditions selected for a compression-absorption heat pump of 100 KW heating capacity are as stated below:

Absorber temperature ( $T_a$ ) = 50-80°C.

Desorber temperature ( $T_d$ ) = 30-40°C in steps of 5.

Desorber pressure ( $p_a$ ) = 4 bar.

Pressure ratio (R) = 5-6.

Heat exchanger effectiveness = 0.50-1

Compressor efficiency = 0.50-1

Pump efficiency = 0.70

## 5.2 Results of First Law Analysis

The results obtained by carrying out the first law analysis of the system has been presented in this section. Various performance parameters that are used to evaluate the system performance based on first law analysis such as coefficient of performance (COP), circulation ratio (CR) etc. have been plotted as a function of absorber temperature, compressor efficiency and heat exchanger effectiveness. The effects of varying these operating parameters on the performance of the system has also been studied in the subsections from 5.2.1 to 5.2.6.

### 5.2.1 Variation of COP with Absorber Temperature

Variation of COP has been studied as a function of the absorber temperature for the various values of desorber temperatures varying in the range of 30-40°C. The results have been plotted and discussed in this section.

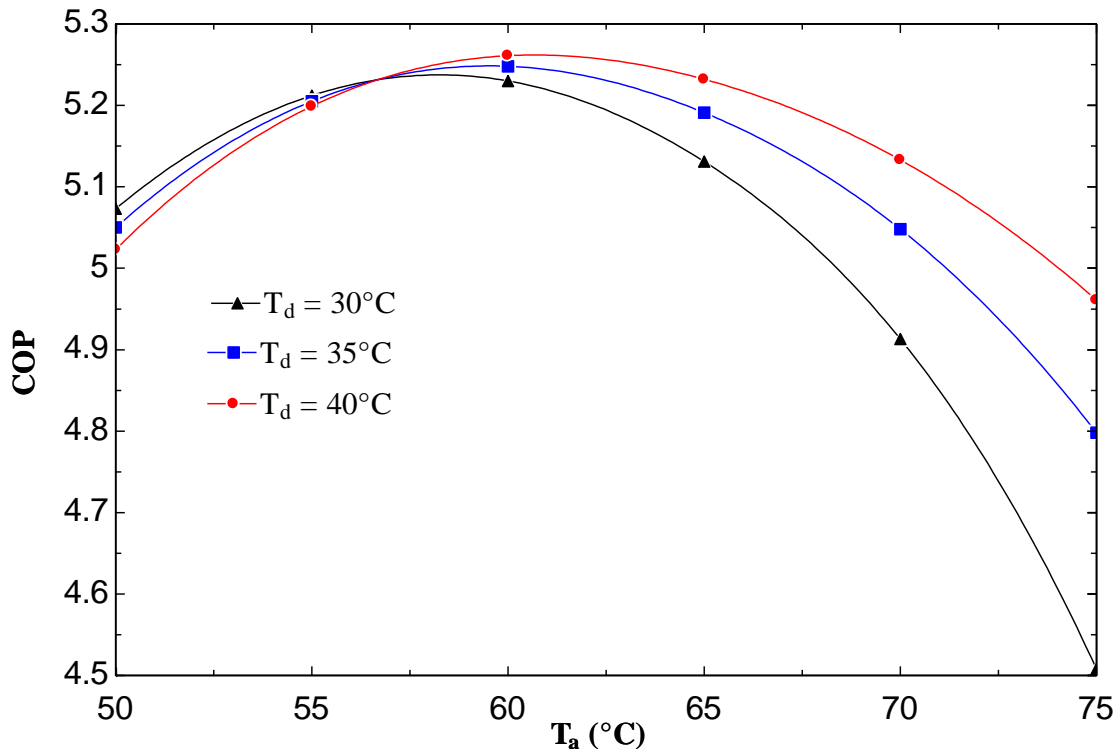


Fig. 5.2.1 Variation of coefficient of performance with absorber temperature.

The variation of COP of the cycle as a function of absorber temperature for various values of desorber temperatures has been shown in Fig. 5.2.1. From Fig. 5.2.1, it is evident that as the absorber temperature increases, COP first increases upto an optimum value of the absorber temperature at which the COP obtained is maximum. With any further increase in the absorber temperature, COP starts decreasing. It is so because as the absorber temperature increases, the mass flow rate of refrigerant decreases which causes a decrease in compressor work, which in turn increases the COP upto the absorber temperature of 60°C. If the absorber temperature is increased further, COP starts decreasing because of an increase in compressor work.

### 5.2.2 Variation of COP with compressor isentropic efficiency

Isentropic efficiency of the compressor has also a considerable effect on the coefficient of performance of the system. The variation of COP as a function of compressor efficiencies has been shown in this section. The absorber temperature of 60°C is selected at which the COP of the system is found to be maximum.

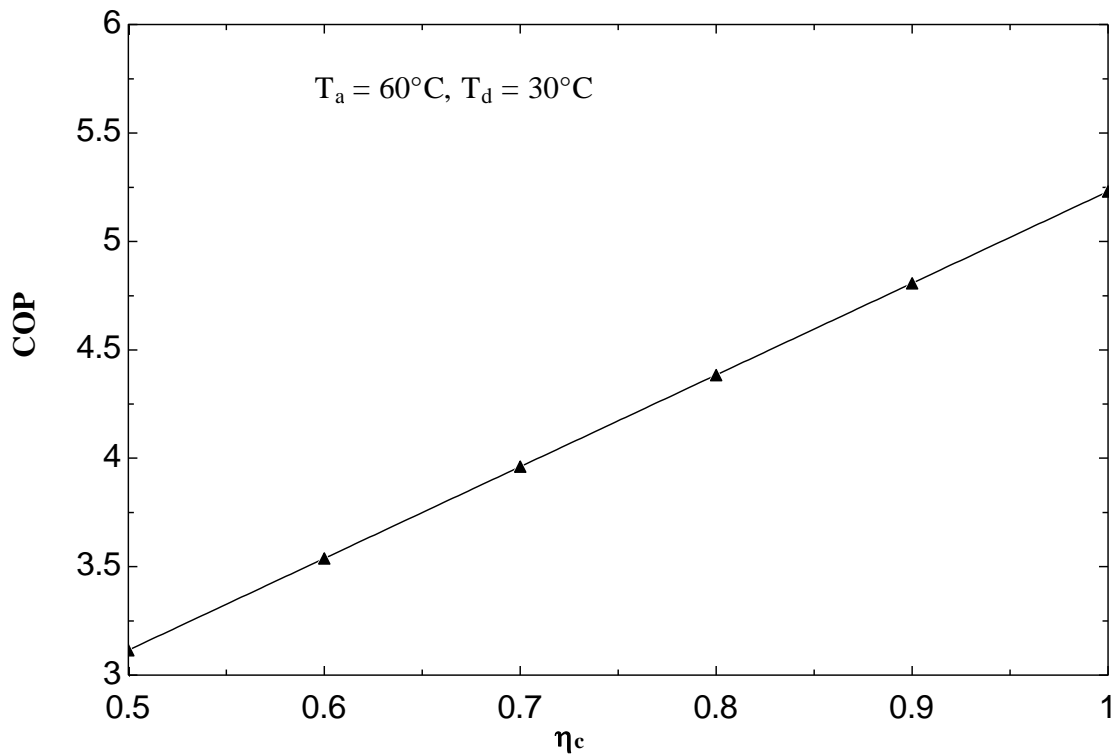


Fig. 5.2.2 Variation of coefficient of performance with compressor efficiency.

It can be seen from Fig. 5.2.2, as the efficiency of the compressor increases the COP also increases due to decrease in the compressor work. Though the pump work has increased but the amount is not significant. It can be seen from Fig. 5.2, on increasing the pressure ratio the COP decreases if all other parameters are fixed. This is due to the fact that as the pressure ratio increases, there is an increase in compressor work which decreases the COP. At a pressure ratio of 5, the COP value corresponding to a compressor efficiency of 0.7, the COP is found to be 3.961 whereas when the pressure ratio has been increased to 6, the COP reduces to 3.471.

### 5.2.3 Variation of COP with effectiveness of solution heat exchanger

Fig. 5.2.3 shows the variation of COP with heat exchanger effectiveness at the absorber temperature of 60°C for the desorber temperature varying in the range of 30-40°C. It can be seen that as the heat exchanger effectiveness increases, the COP also increases for a constant value of desorber temperature.

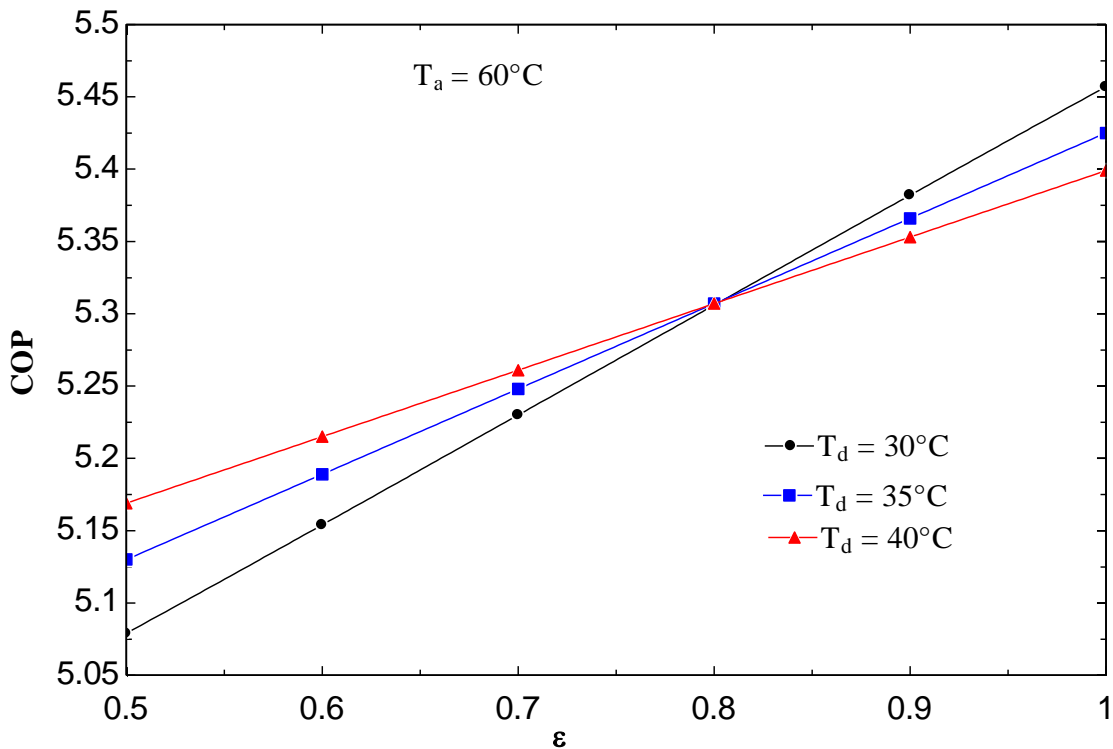


Fig. 5.2.3 Variation of coefficient of performance with heat exchanger effectiveness

Upto the effectiveness of 0.8, the COP is more for a higher value of desorber temperature. At heat exchanger effectiveness of 0.8, COP is found to be 5.3 for all the desorber temperatures. For the heat exchanger effectiveness more than 0.8, COP is more at a lower value of desorber temperature. At low values of heat exchanger effectiveness COP is less. This is due to increase in weak solution concentration and mass flow rate of the refrigerant which increases the net work input and as a result of which the COP decreases. At higher values of heat exchanger effectiveness, both the compressor and the pump work decrease hence COP increases. For a high solution flow rate, corresponding to a small absorber glide, the solution heat exchanger becomes very important as the amount of energy to be transferred between the strong and the weak solution is large.

#### 5.2.4 Variation of compressor work with absorber temperature.

The variation of the work input to the compressor with the absorber temperature has been presented in this section. The curve has been plotted at the desorber temperature of 30°C.

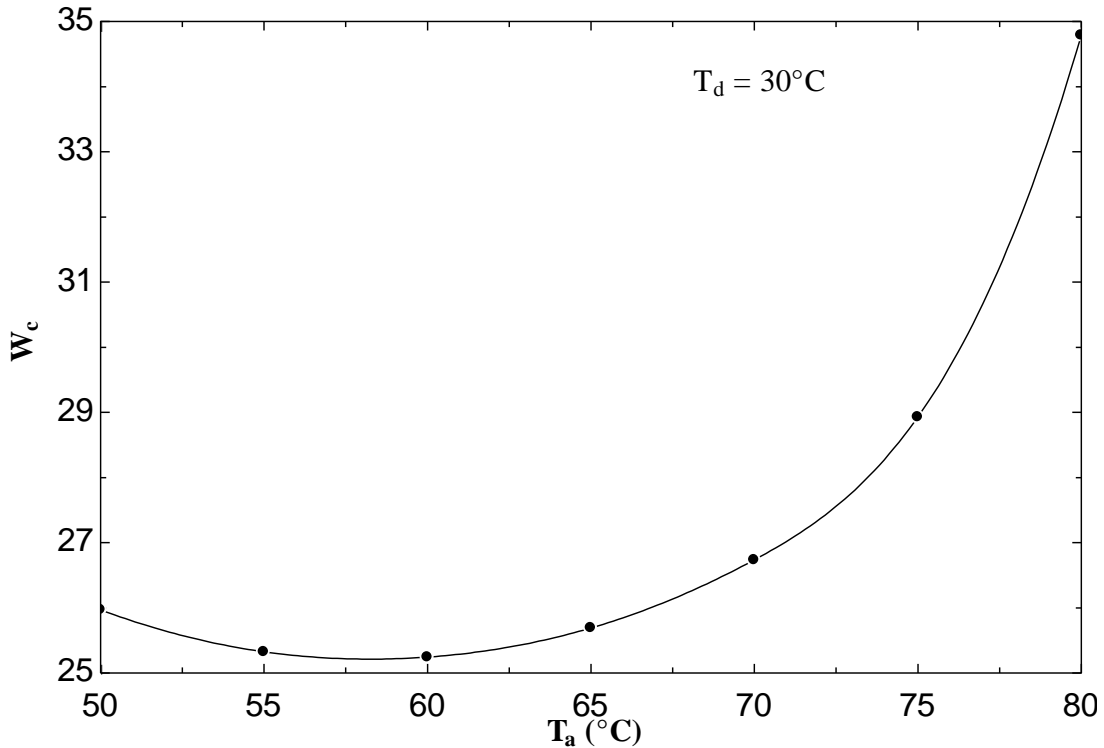


Fig. 5.2.4 Variation of compressor input power with absorber temperature.

As shown in Fig. 5.2.4 , the compressor power first decreases with an increase in absorber temperature, becomes minimum at a particular point which for the operating conditions selected for the present study is at an absorber temperature of 60°C for a desorber temperature of 30°C. With any further increase in the absorber temperature, the compressor work starts increasing. At a fixed value of absorber temperature, the compressor work is more for low weak solution concentration.

### 5.2.5 Variation of Circulation Ratio with absorber temperature

The circulation ratio (CR) is very important factor for the performance of the cycle as it governs the losses in the solution circuit and the pump work. At high weak solution concentration, the circulation ratio is low.

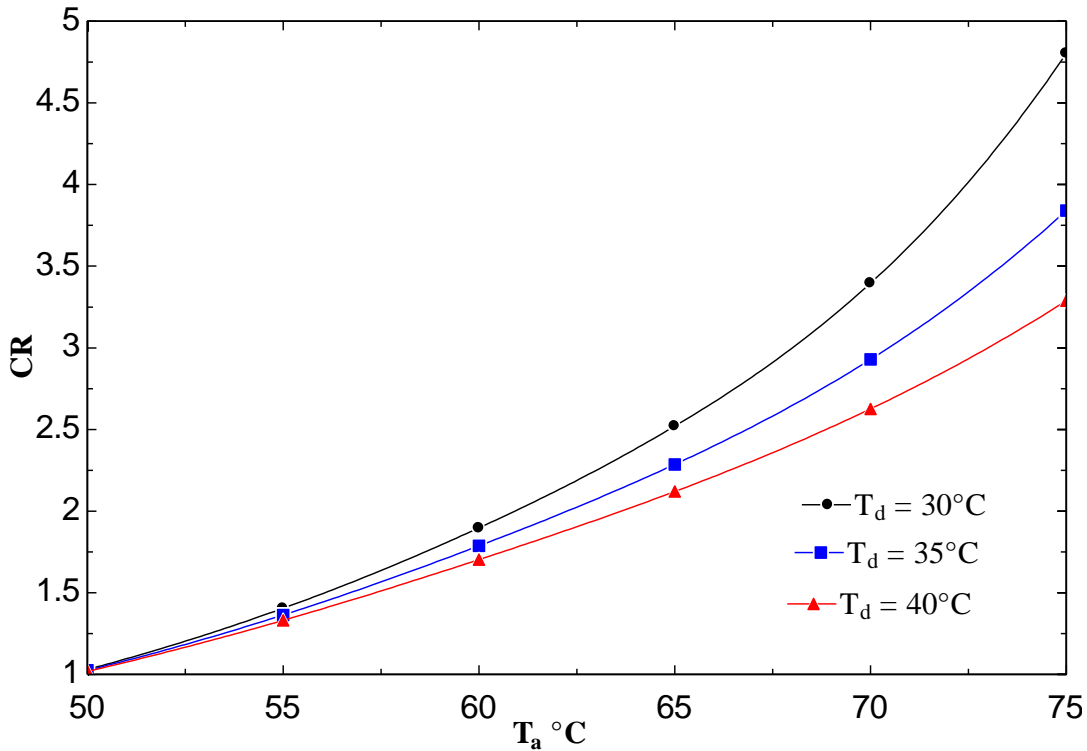


Fig. 5.2.5 Variation of circulation ratio with absorber temperature.

Fig. 5.2.5 shows that as the absorber temperature increases, circulation ratio increases at constant values of compression ratio and the desorber temperature. As the absorber temperature is increased, the mass flow rate of strong solution increases which results in an increase in the circulation ratio. It can also be explained as that on increasing the absorber

temperature, the equilibrium concentration of strong solution reduces. This results in lesser concentration width and consequently a higher circulation ratio. It can be seen from the fig. that at a constant value of absorber temperature, the circulation ratio is less at a higher value of desorber temperature. The reason for this is that as the desorber temperature is increased, weak solution concentration decreases which results in an increase in concentration width, hence the circulation ratio decreases.

### 5.2.6 Variation of Concentration Width with Absorber Temperature

The variation of the concentration width with absorber temperature corresponding to three values of desorber temperatures i.e. at 30°C, 35°C and 40°C has been shown in this section. Concentration width is the difference between the strong and the weak solution concentrations.

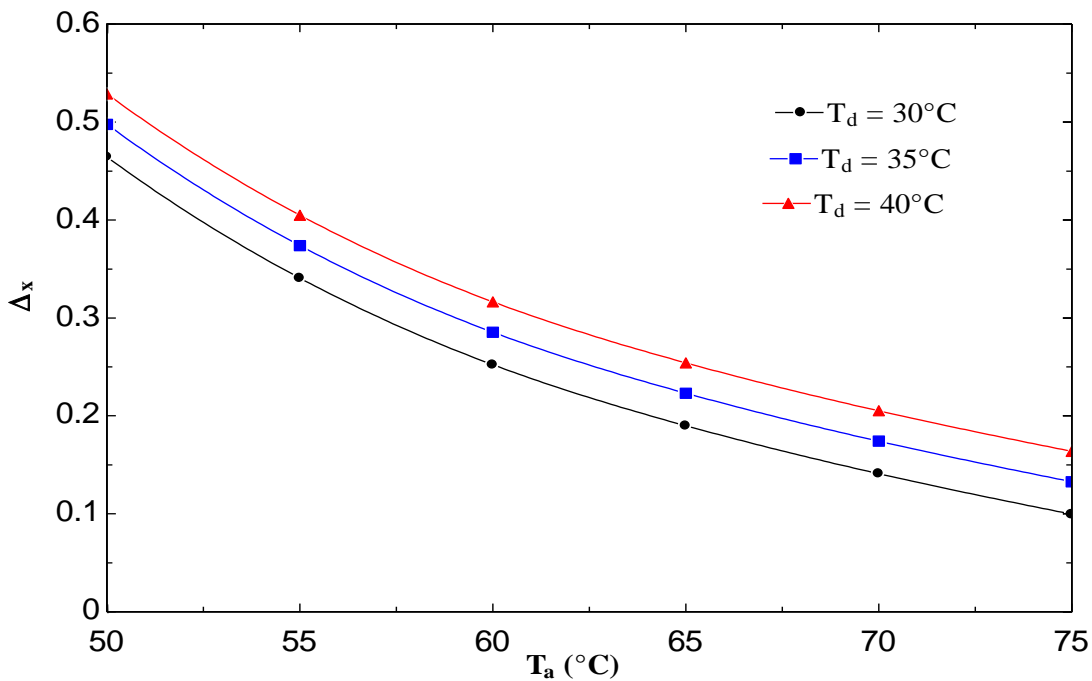


Fig. 5.2.6 Variation of concentration difference with absorber temperature.

In Fig. 5.2.6, it is shown that as the absorber temperature is increased, at a constant value of absorber pressure, the strong solution concentration increases with the weak solution concentration remaining constant. This causes the concentration difference between the



strong and the weak solution to decrease. As the desorber temperature is increased, the concentration width increases due to decrease in the weak solution concentration.

A sharper picture of the performance is provided by the results of the exergetic analysis. The exergy analysis emphasizes that both losses and irreversibility have an impact on system performance. The inlet and the outlet exergy of any process do not match. The difference represents the exergy lost during that process. An exergy analysis is performed to determine the potential areas of improvement in the cycle.

### **5.3 Results of Second Law Analysis**

The results of second law analysis of the system have been presented in this section. From the second law analysis of the system, both the individual component exergy loss and the non dimensional exergy loss have been calculated. The performance parameters used to evaluate the system from exergetic point of view are the exergetic efficiency and the exergy destruction ratio. Exergy destruction ratio (EDR) helps to predict the contribution of a component to the total exergy loss so that the component with higher values can be improved. The variation of exergetic efficiency of the system with absorber temperature, compressor efficiency and heat exchanger effectiveness and the exergy destruction ratio of all the components of the system has been shown and discussed in the subsections from 5.3.1 to 5.3.10. In Table II of Appendix I, a comparative picture of exergy losses in various system components reveal that if the highest exergy loss occurs in the absorber. It is found that for the same set of operating conditions, the exergy loss in the absorber is the highest. At an absorber temperature of 60°C and desorber temperature of 30°C, 38.06% of the total exergy loss is contributed by the absorber. It can also be seen that the next highest exergy loss occurs in the compressor which is equal to 30.62% which is followed by the exergy loss in the desorber, expansion valve, pump and the solution heat exchanger.

#### **5.3.1 Variation of exergetic efficiency with absorber temperature**

The variation of exergetic efficiency with absorber temperature at various values of desorber temperatures i.e. at 30°C, 35°C and 40°C keeping all the other parameters as constant has been shown and discussed in this section.

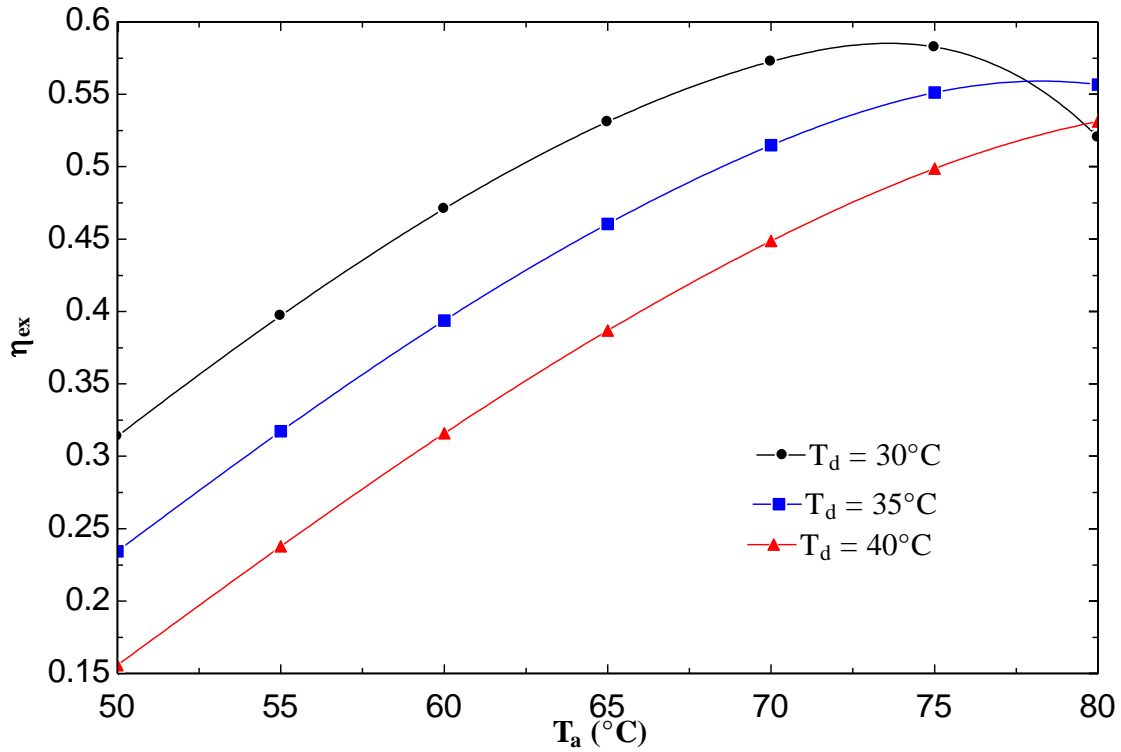


Fig. 5.3.1 Variation of exergetic efficiency with absorber temperature ( $T_d = 30^\circ\text{C}$ ,  $35^\circ\text{C}$ ,  $40^\circ\text{C}$ )

It can be seen from Fig. 5.3.1, as the absorber temperature is increased, the exergetic efficiency is increased for a constant value of desorber temperature because it increases the

term  $\left(1 - \frac{T_d}{T_a}\right)$  in the expression for exergetic efficiency as stated by equation 3.49 in chapter

3. The compressor work decreases and the pump work increases but the rate of increase of the pump work is small, hence the exergetic efficiency increases. With an increase in the

desorber temperature, the term  $\left(1 - \frac{T_d}{T_a}\right)$  and pump work decreases causing a decrease in the

exergetic efficiency. From Fig. 5.3.1, it is seen that the exergetic efficiency is maximum at an absorber temperature of  $75^\circ\text{C}$  corresponding to a desorber temperature of  $30^\circ\text{C}$  which is equal to 0.4467. For higher values of desorber temperature, the peak of the curve shifts to the right.

### 5.3.2 Variation of exergetic efficiency with heat exchanger effectiveness.

In this section, the variation of exergetic efficiency has been plotted as a function of heat exchanger effectiveness. The curve has been drawn for fixed values of absorber temperature, compressor efficiency and pressure ratio. The absorber temperature, compressor efficiency and pressure ratio are taken as  $60^{\circ}\text{C}$ ,  $0.7$  and  $5$  respectively. The variation has been shown corresponding to the desorber temperatures of  $30^{\circ}\text{C}$ ,  $35^{\circ}\text{C}$  and  $40^{\circ}\text{C}$ .

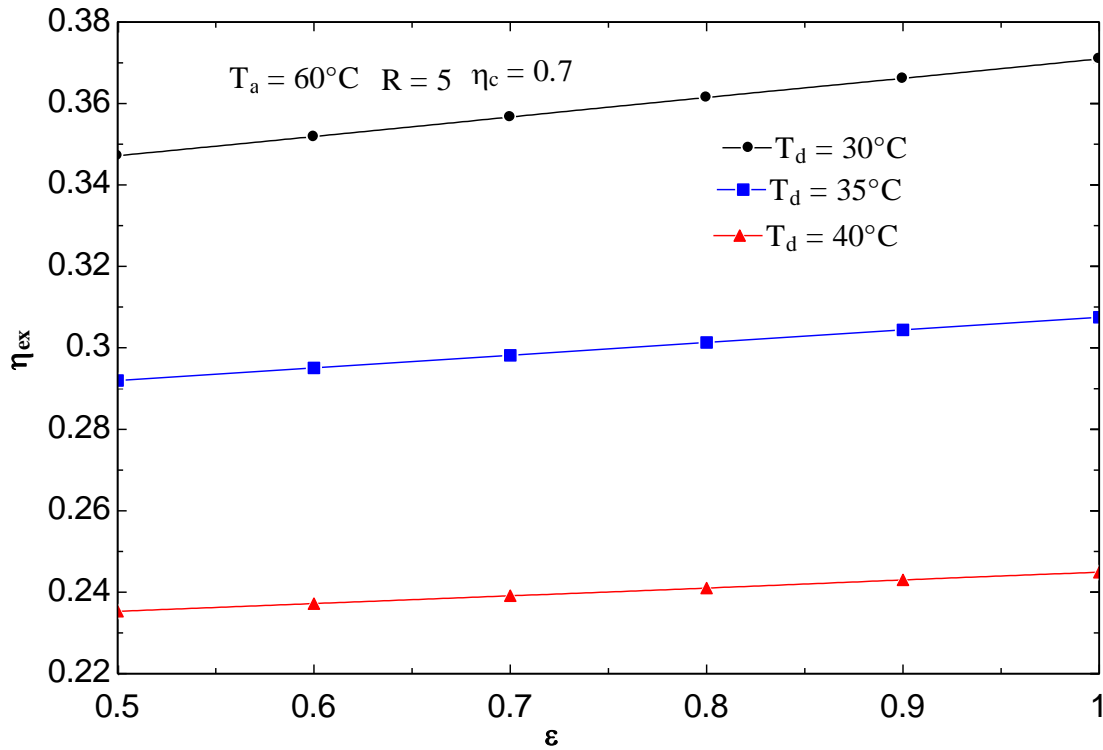


Fig. 5.3.2 Variation of exergetic efficiency with heat exchanger effectiveness

Fig. 5.3.2 shows that on increasing the effectiveness of solution heat exchanger, the exergetic efficiency of the system also increases at a constant value of desorber temperature. For higher values of desorber temperatures, the exergetic efficiency is more at a fixed value of heat exchanger effectiveness.

### 5.3.3 Variation of exergetic efficiency with compressor efficiency

Compressor efficiency also affects the exergetic efficiency of this system. The variation of exergetic efficiency with the compressor efficiency has been shown in Fig. 5.3.3. From the fig, it can be seen that on increasing the compressor efficiency the exergetic efficiency also increases. The absorber and desorber temperatures are kept fixed at 75°C and 30°C respectively.

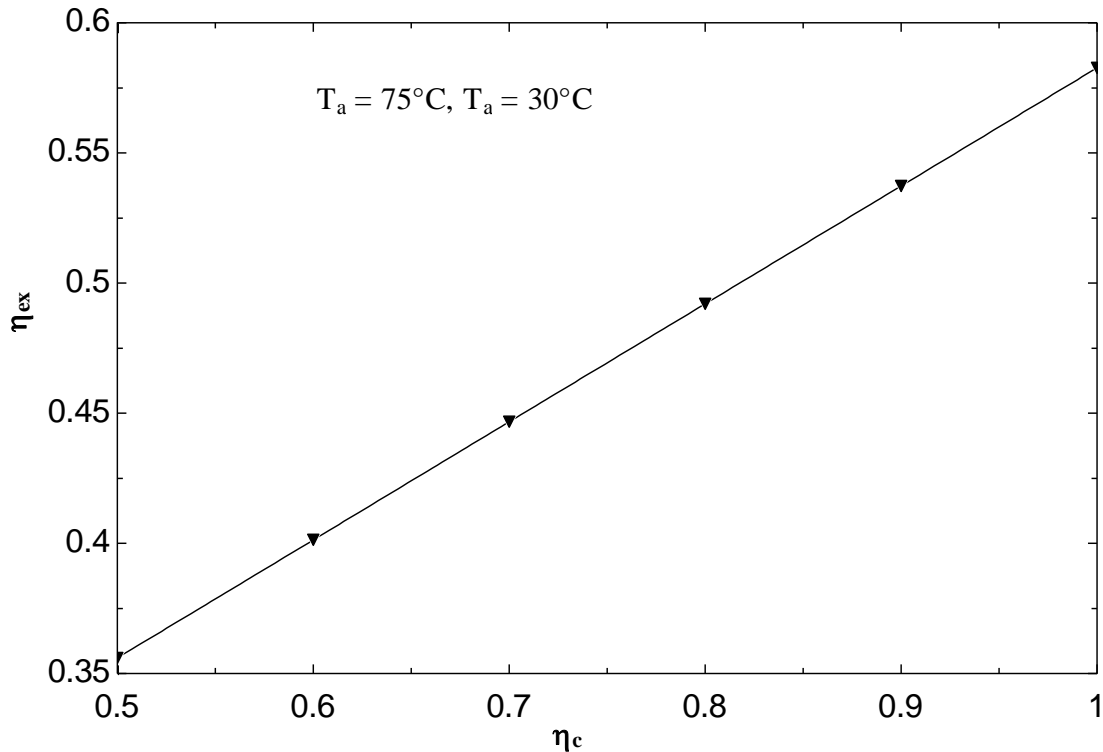


Fig. 5.3.3 Variation of exergetic efficiency with compressor efficiency

Since the heating capacity is also fixed, the numerator of the expression for exergetic efficiency of the system as given by eqn. 3.49 remains constant. With an increase in compressor efficiency, compressor input power reduces which leads to an increase in the exergetic efficiency of the system.

### 5.3.4 Variation of Exergy destruction ratio in the absorber ( $EDR_a$ ) with absorber temperature.

A comparative picture of exergy losses in various system components reveals that the highest exergy loss occurs in the absorber. This section presents the variation of exergy

destruction ratio in the absorber as a function of absorber temperature at various values of desorber temperature. The heat exchanger effectiveness, compressor efficiency and pressure ratio are fixed at the values of 0.7, 0.7, 5 respectively. For a particular set of operating conditions, absorber has the highest exergy destruction ratio. As can be seen from Fig. 5.3.4, as the absorber temperature is increased, the exergy destruction in the absorber reduces for a fixed value of desorber temperature. At a fixed absorber temperature,  $EDR_a$  is more at a higher value of desorber temperature. For a fixed value of reference temperature and the absorber heat load, the thermal exergy loss component as stated in Eqn. 3.39 increases with an increase in absorber temperature which in turn increases the exergy loss in the absorber.

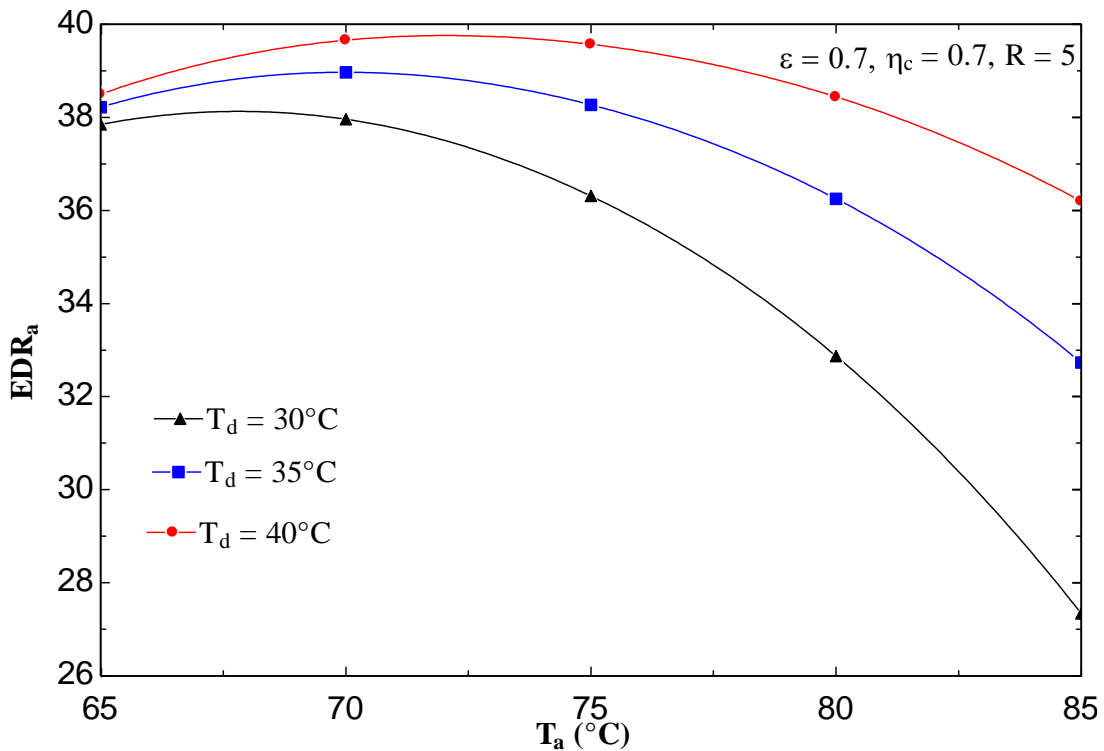


Fig. 5.3.4 Variation of Exergy Destruction Ratio in the absorber with absorber temperature.

### 5.3.5 Variation of Exergy destruction ratio in the compressor ( $EDR_c$ ) with absorber temperature.

Exergy destruction ratio in the compressor has the second highest value for a similar set of operating conditions. From Fig. 5.3.5, it is observed that on increasing the absorber temperature, exergy destruction ratio of compressor first increases upto an absorber temperature at which it becomes maximum which then starts decreasing with any further

increase in the absorber temperature. The higher the desorber temperature is, the lesser is the exergy destruction in the compressor due to the reduction in the temperature difference of heat transfer.

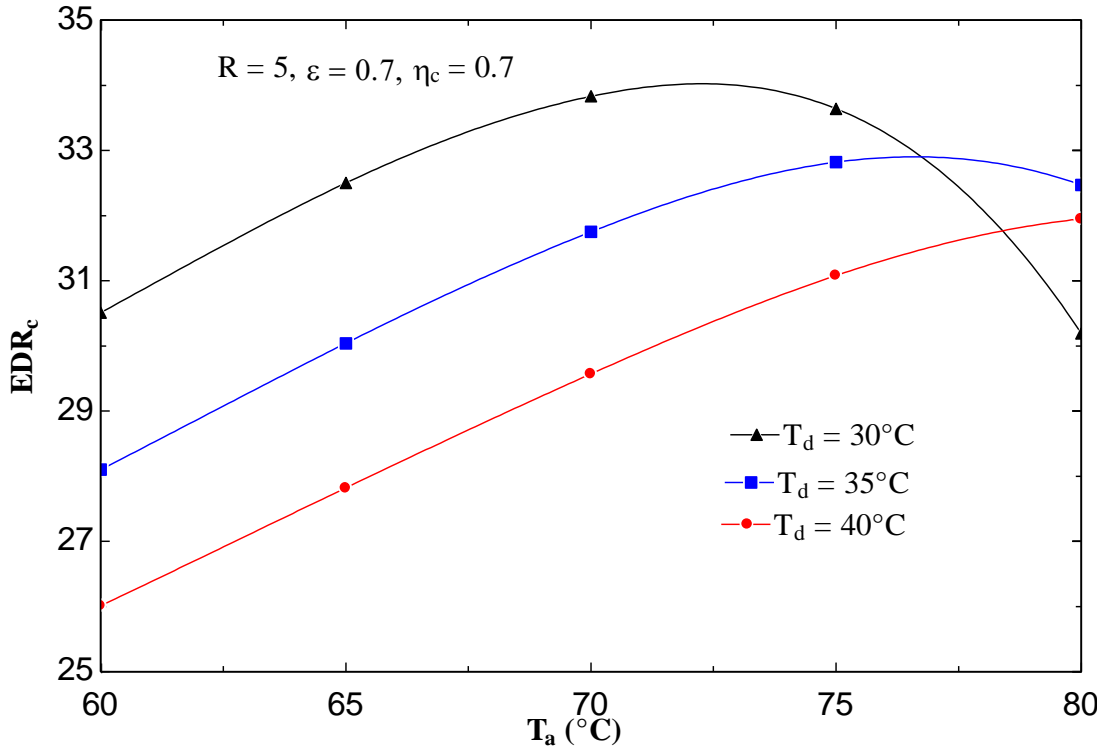


Fig. 5.3.5 Variation of Exergy Destruction Ratio in the compressor with absorber temperature.

Compressor isentropic efficiency also affects the exergy destruction ratio in the compressor. As seen from Fig. 5.3.5, as the compressor efficiency is increased, the exergy destruction ratio of the compressor decreases if all the other parameters are kept constant. On increasing the absorber temperature, the mass flow rate of the refrigerant increases thus increasing the exergy destruction in the compressor.

**5.3.6 Variation of Exergy Destruction Ratio in compressor with compressor efficiency.**

This section presents the variation of the exergy destruction ratio in the compressor as a function of compressor efficiency. Fig. 5.3.6 shows the effect of compressor efficiency on the exergy destruction in the compressor. As it can be seen from the figure, as the compressor efficiency is increased, the exergy destruction in the compressor reduces. This is

due to the fact that as the compressor efficiency is increased, the power input to the compressor reduces and consequently the exergy destruction in the compressor also reduces.

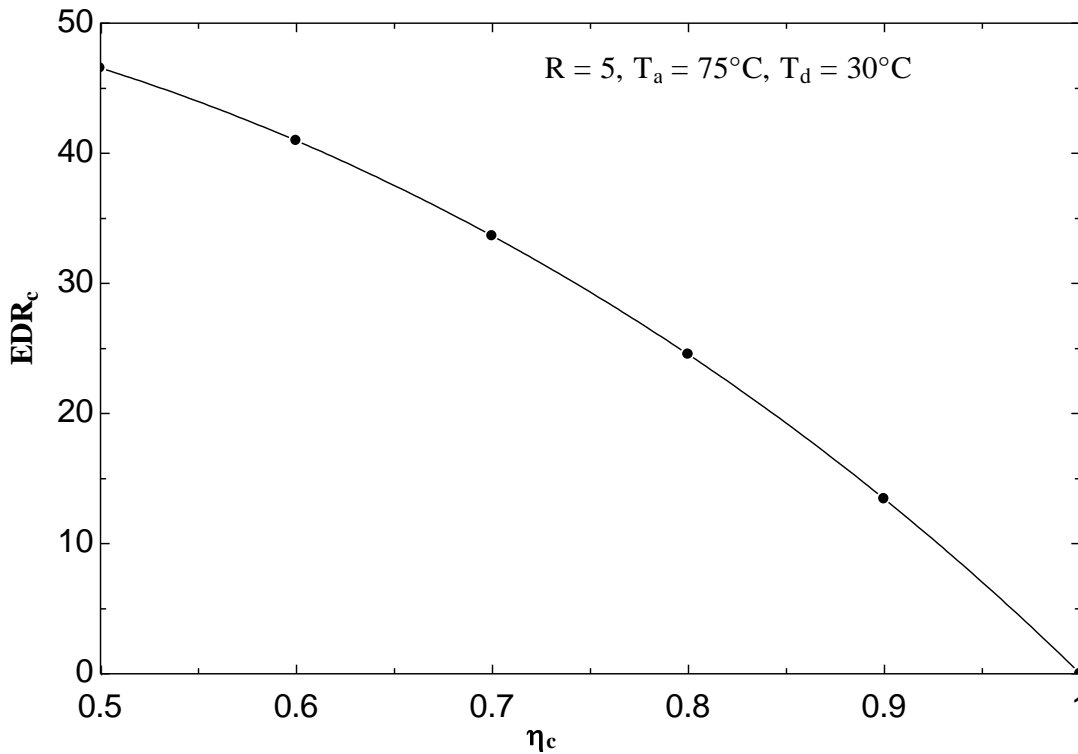


Fig. 5.3.6 Variation of Exergy Destruction Ratio in the compressor with compressor efficiency.

### 5.3.7 Variation of Exergy Destruction Ratio in desorber ( $EDR_d$ ) with absorber temperature

The variation of exergy destruction ratio in the desorber with absorber temperature has been discussed in this section. The values of pressure ratio, compressor efficiency and heat exchanger effectiveness have been fixed at 5, 0.7 and 0.7 respectively. These variations have been plotted corresponding to the desorber temperatures of 30°C, 35°C and 40°C. The reason for the exergy destruction in the desorber is the heat transfer through a finite temperature difference. The exergy destruction ratio in the desorber for the selected set of operating conditions is found to be third highest. As the absorber temperature is increased, the  $EDR_d$  decreases at a constant value of desorber temperature. On increasing the desorber temperature,  $EDR_d$  also increases.

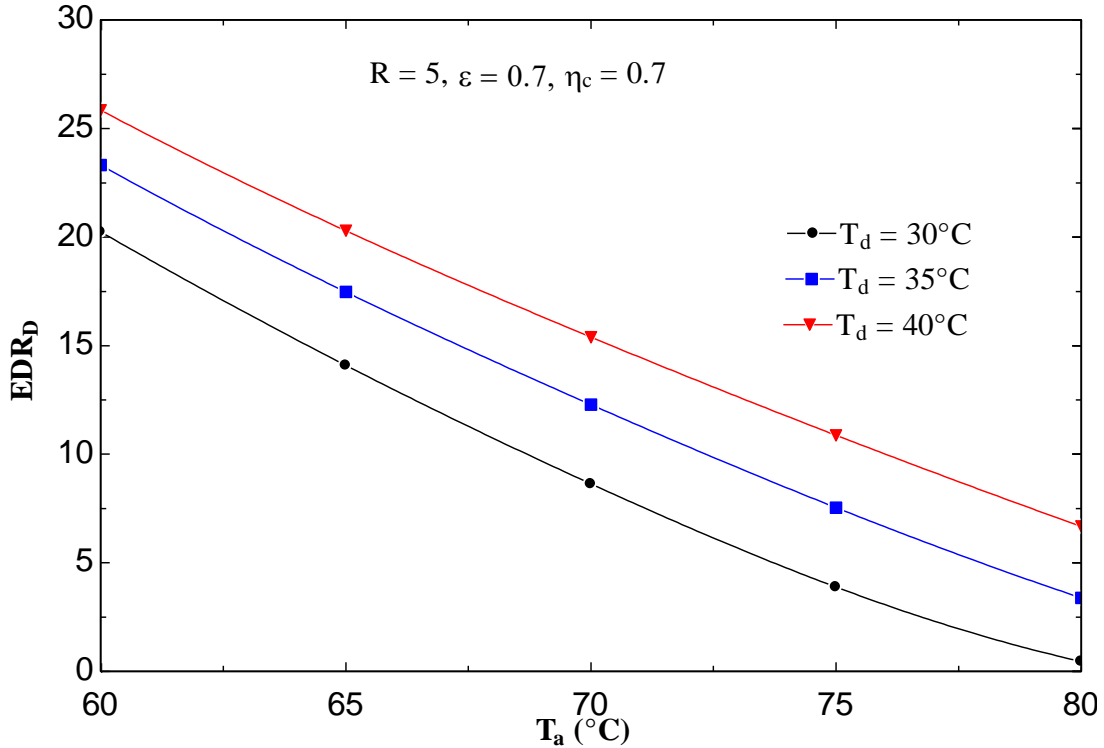


Fig. 5.3.7 Variation of Exergy Destruction Ratio in the desorber with absorber temperature at various desorber temperatures ( $T_d = 30^\circ\text{C}$ ,  $35^\circ\text{C}$  and  $40^\circ\text{C}$ )

### 5.3.8 Variation of Exergy Destruction Ratio in Expansion valve (EDR<sub>ev</sub>) with absorber temperature.

In this section, the variation of exergy destruction ratio of the expansion valve with absorber temperature has been shown at the desorber temperatures of  $30^\circ\text{C}$ ,  $35^\circ\text{C}$  and  $40^\circ\text{C}$ . The contribution of the exergy loss in the expansion valve to the total exergy loss of the system is small. The variation of exergy destruction ratio in the expansion valve has been shown in Fig. 5.3.8 at various values of desorber temperature. Compressor efficiency, heat exchanger effectiveness and pressure ratio values have been fixed as 0.7, 0.8 and 5 respectively. It is evident from the curve that as the absorber temperature is increased, the mass flow rate of strong solution entering the expansion valve increases which in turn increases the exergy loss in the expansion valve. As the desorber temperature is increased, the exergy loss in the expansion valve is reduced.



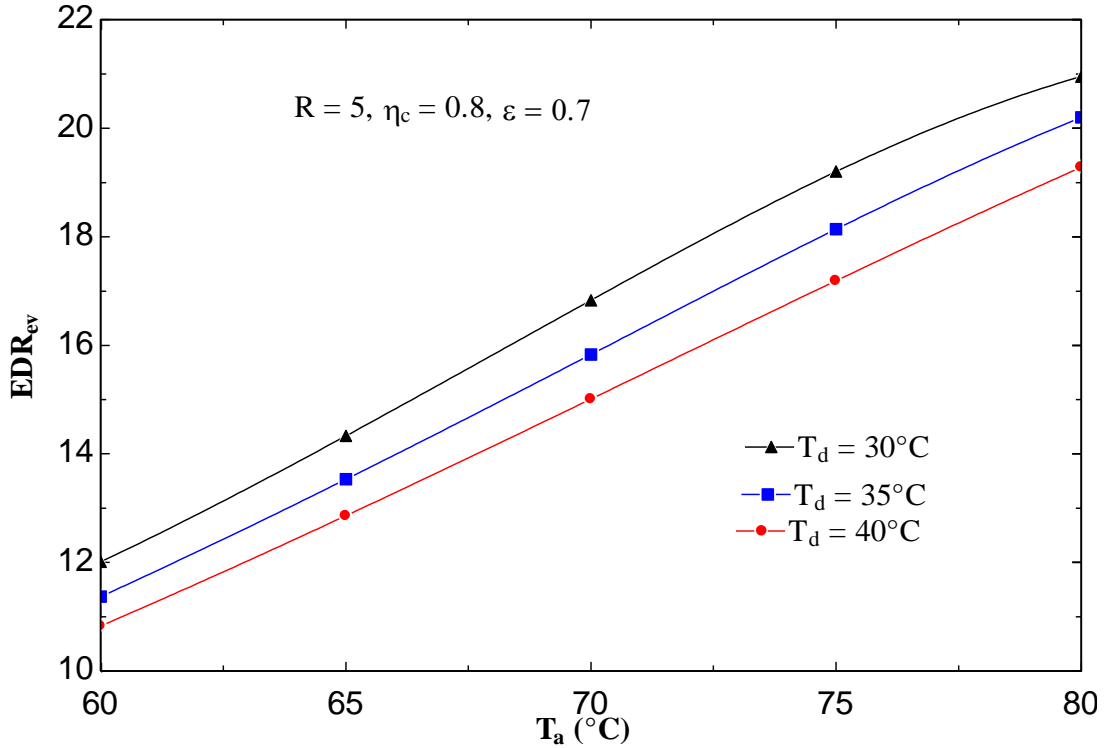


Fig. 5.3.8 Variation of Exergy Destruction Ratio in the expansion valve with absorber temperature.

### 5.3.9 Variation of Exergy Destruction Ratio of Expansion valve (EDR<sub>ev</sub>) with heat exchanger effectiveness.

This section discusses the variation of exergy destruction ratio of the expansion valve as a function of solution heat exchanger effectiveness. The variation of exergy destruction ratio of expansion valve with effectiveness of solution heat exchanger has been shown in Fig. 5.3.9. The curve has been drawn at the absorber and desorber temperatures of 60°C and 35°C respectively. The compression efficiency is taken as 0.7. As can be seen from the figure, as the effectiveness of heat exchanger increases, the exergy destruction in the solution heat exchanger decreases. Its contribution to the total exergy loss in the system is also very less. Table II shows that for the same set of operating conditions, 9.474% of the total exergy loss in the system is contributed by the expansion valve.

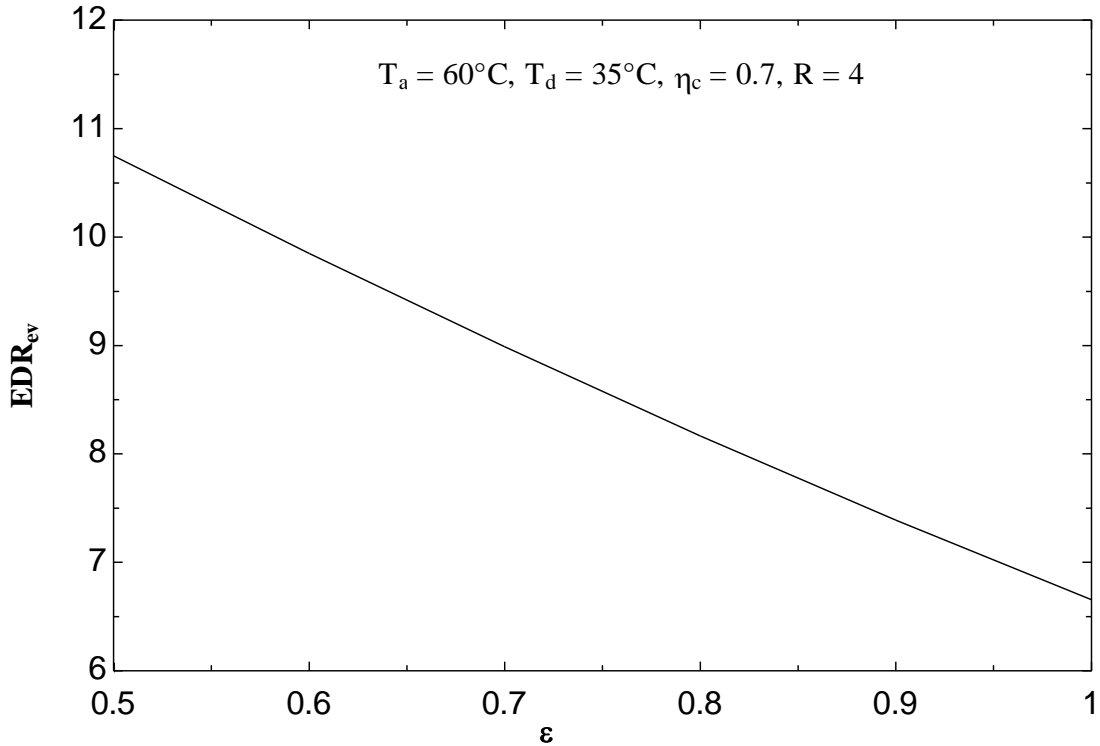


Fig. 5.3.9 Variation of Exergy Destruction Ratio in the expansion valve with heat exchanger effectiveness.

The contribution of the pump and the solution heat exchanger to the overall exergy loss of the system is marginal. At the absorber temperature and desorber temperatures Therefore, the variation of exergy loss in the pump and solution heat exchanger have been studied with absorber temperature only corresponding to the desorber temperatures of 30, 35 and 40°C.

### 5.3.10 Variation of Exergy Destruction Ratio in solution pump ( $EDR_p$ ) with absorber temperature.

The variation of exergy destruction ratio of the solution pump with absorber temperature has been shown in this section. The contribution of the pump exergy loss is very less. From Table II of Appendix I, it can be seen that at an absorber temperature of 60°C and desorber temperature of 30°C ,the exergy loss contributed by the solution pump is only 0.7013%. It can be seen from Fig. 5.3.10, as the absorber temperature is increased , the exergy destruction ratio of the pump also increases at a constant value of desorber temperature.

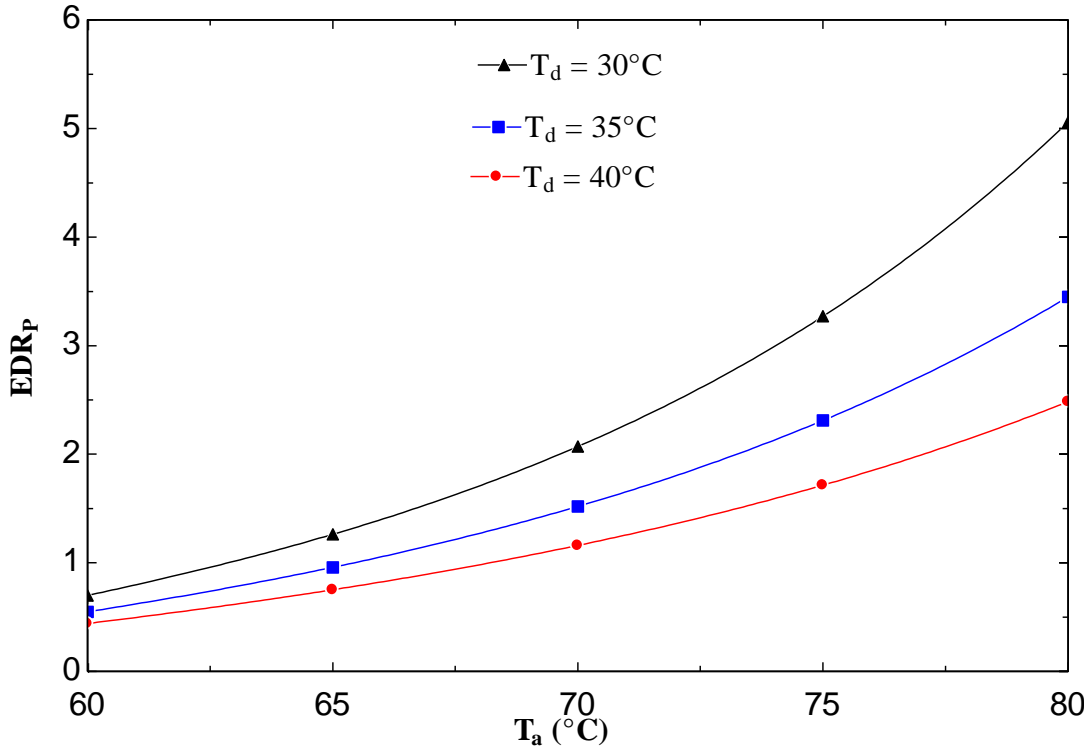


Fig. 5.3.10 Variation of Exergy Destruction Ratio in the solution pump with absorber temperature.

As it is shown in Fig. 5.3.10, with an increase in absorber temperature, the exergy loss in the pump also increases at a constant value of desorber temperature. With an increase in absorber temperature, the mass flow rate of weak solution entering the absorber increases which also increases the pump work. Consequently, the exergy loss in the absorber also increases. As the desorber temperature is increased, the exergy destruction in the pump is reduced.

### 5.3.11 Variation of Exergy Destruction Ratio in solution heat exchanger ( $\text{EDR}_{\text{shx}}$ ) with absorber temperature.

In this section, the variation of exergy destruction ratio in the solution heat exchanger has been shown as a function of absorber temperature. The contribution of the exergy loss in the solution heat exchanger to the total exergy loss of the system is least significant as can be seen from Table II of Appendix I. For the similar set of operating conditions as mentioned in section 5.3.10, only 0.5261% of the total exergy loss is contributed by the solution heat

exchanger. The variation of the exergy destruction ratio in the solution heat exchanger as a function of absorber temperature is shown in Fig. 5.3.11.

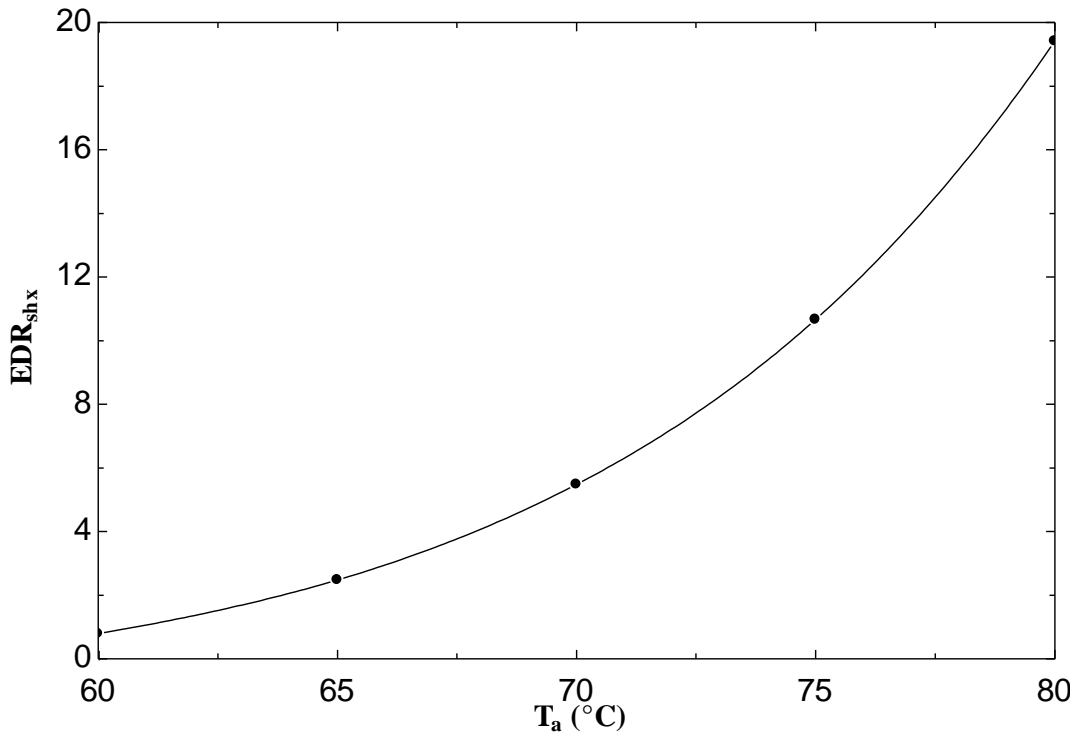


Fig. 5.3.11 Variation of Exergy Destruction Ratio in the solution heat exchanger with absorber temperature.

It can be seen from Fig. 5.3.11 that on increasing the absorber temperature, the exergy loss in the solution heat exchanger also increases.

#### 5.4 Analysis of High temperature Lift Compression-Absorption Heat Pump

In some industrial processes where waste heat is available at temperatures 50-60°C compression absorption heat pumps can be used to further raise the temperatures upto 100°C or above for some high temperature applications. The results of first and second law analysis of compression absorption heat pumps for such large range of temperatures have been presented in this section.

##### 5.4.1 Variation of COP with absorber temperature.

If the heat source is available at a temperature of 50°C, a compression-absorption heat pump can be used to lift the temperature above 100°C using ammonia-water mixture. The

variation of the coefficient of performance (COP) of the heat pump with absorber temperature has been shown in Fig. 5.4.1. The desorber and the absorber pressures are chosen to be 4 bar and 24 bar respectively, which makes the pressure ratio as 4.

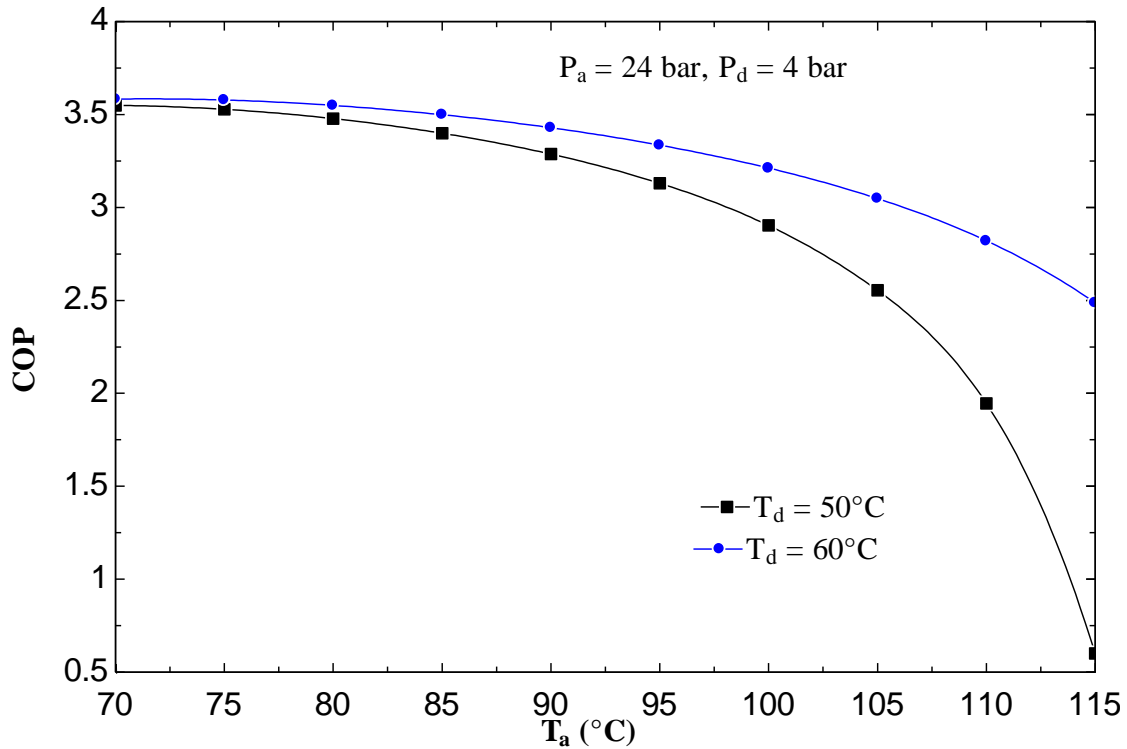


Fig. 5.4.1 Variation of COP with absorber temperature.

From Fig. 5.4.1, it is observed that a temperature lift from  $50^{\circ}\text{C}$  to  $115^{\circ}\text{C}$  is possible using an ammonia-water compression-absorption heat pump when it is operated at the above mentioned set of operating conditions. It can also be seen that as the absorber temperature is increasing, the COP decreases at a constant value of desorber temperature. The COP is more at a higher value of desorber temperature for each absorber temperature. As seen from the Fig.5.4.1, at an absorber temperature of  $70^{\circ}\text{C}$ , a COP of 3.549 is obtained when the desorber temperature is  $50^{\circ}\text{C}$  and when the desorber temperature is increased to  $60^{\circ}\text{C}$ , COP is increased to 3.583. To further raise the temperature beyond  $115^{\circ}\text{C}$ , the pressure ratio has to be increased by keeping the other parameters as fixed.

### 5.4.2 Variation of COP with compressor efficiency

The variation of COP with isentropic efficiency of the compressor has been shown in Fig. 5.4.2. The curve is plotted for two values of pressure ratio i.e. 5 and 6. As can be seen from

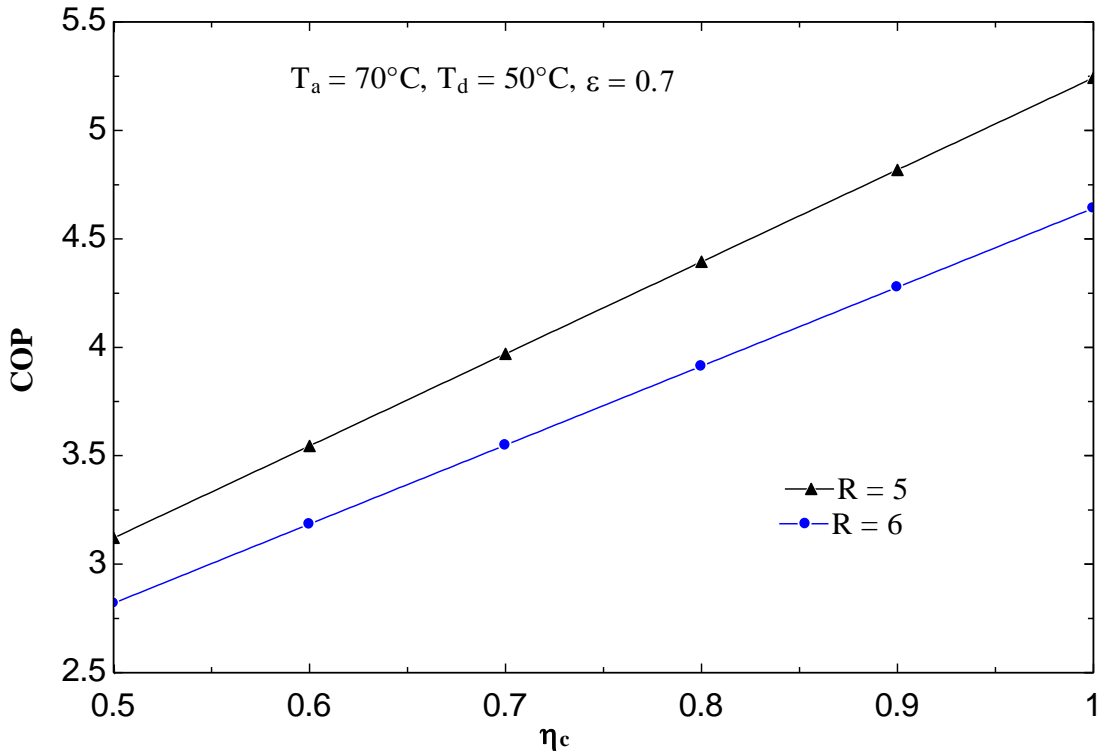


Fig. 5.4.2 Variation of COP with compressor efficiency

the Fig. 5.4.2, as the compressor efficiency is increased, the COP also increases. This is due to the decrease in the compressor work. Though the pump work has increased but the amount is not significant. To increase the further temperature lift i.e. above  $105^\circ\text{C}$ , the pressure ratio needs to be increased. On raising the pressure ratio from 5 to 6, the temperature of the heat pump considered could be increased upto  $120^\circ\text{C}$  but at a lower COP. For example, at an absorber temperature of  $70^\circ\text{C}$  and a desorber temperature of  $50^\circ\text{C}$ , a COP of 3.97 and 3.549 are obtained for pressure ratios of 5 and 6 respectively.

### CONCLUSIONS

Through a comprehensive energy and exergy analysis of the compression-absorption heat pump of 100 kW heating capacity considered in the present study, following conclusions can be drawn:

1. Computer simulations of the compression-absorption cycle showed that for every application, a value of the absorber temperature which maximizes the COP of the cycle can be determined. In the present work, at an absorber pressure of 20 bar and desorber pressure of 4 bar, the maximum value of COP is obtained corresponding to an absorber temperature of  $60^{\circ}\text{C}$  which is equal to 3.988.
2. On increasing the absorber temperature, keeping other parameters as constant, the COP of the heat pump first increases till it reaches an optimum value, which then starts decreasing with a further increase in the absorber temperature.
3. Exergy efficiency values of the system were found to range from 35.67% to 40.68% at the absorber temperatures varying from 60 to  $80^{\circ}\text{C}$
4. Exergetic efficiency of the system first increases with an increase in absorber temperature, reaches a maximum value which then starts decreasing with a further increase in the absorber temperature. On increasing the compressor efficiency and the heat exchanger effectiveness, the exergetic efficiency of the system increases.
5. The highest exergy loss occurred in the absorber followed by compressor, desorber, expansion valve, pump and solution heat exchanger.
6. Based on the comparative analysis of the exergy destruction ratio of all the components of the system, it can be concluded that the contribution of the exergy loss in the absorber to the total exergy loss is the highest. At an absorber temperature of  $60^{\circ}\text{C}$  and a desorber temperature of  $30^{\circ}\text{C}$ , approximately 38.06% of the total exergy loss has been contributed by the absorber.
7. The second highest exergy loss equal to 30.62% for the similar set of operating conditions has occurred in the compressor which first increases upto a maximum value with an increase in absorber temperature and then starts decreasing with a

further increase in the absorber temperature. At a higher value of desorber temperature, lower is the exergy destruction in the compressor. On increasing the isentropic efficiency of the compressor, the exergy destruction ratio of the compressor is reduced.

8. The exergy destruction ratio of the desorber is found to be approximately 20.62% which is the third highest value among the exergy destruction ratios of all the system components. The exergy loss in the desorber decreases with an increase in absorber temperature.
9. The contribution of the exergy losses in the expansion valve, solution pump and the solution heat exchanger to the total exergy loss of the system is marginal. At the absorber temperature and desorber temperature of 60°C and 30°C respectively, the exergy destruction ratios in the expansion valve, pump and solution heat exchanger are 9.474%, 0.7013% and 0.5261% respectively. For all the three components, the exergy loss increases with an increase in the absorber temperature.
10. The temperature lift of the system can be increased by increasing the absorber pressure thus increasing the pressure ratio. When the pressure ratio is increased from 5 to 6, the temperature of the absorber has been raised to 115°C but with a lower COP.



## Appendix I

Table I : Thermodynamic properties used for the exergetic calculations of the NH<sub>3</sub>-H<sub>2</sub>O mixture at various state points of the cycle. ( R=5, T<sub>d</sub>=30°C)

State point	T (K)	p (bar)	x (kg/kg)	h (kJ/kg)	s (kJ/kgK)	m (kg/s)
1	303.1	4	0.9973	1347	4.941	0.06833
2	434.4	20	0.9973	1621	4.941	0.06833
2n	479.1	20	0.9973	1739	5.198	0.06833
3	303.1	4	0.5188	-104.8	0.2909	0.1637
4	302.8	20	0.5188	-104.8	0.2846	0.1637
5	337	20	0.5188	49.89	0.7685	0.1637
6	343.1	20	0.6597	116.2	0.8982	0.2321
7	320.2	20	0.6597	7.04	0.569	0.2321
8	290.4	4	0.6597	7.04	0.5996	0.2321

Table II : Exergy loss rates of the various components of the system.(T<sub>a</sub> = 60°C, T<sub>d</sub> = 30°C,R=5)

Components	Exergy loss rate(kW)	Non-dimensional exergy loss(%)
Absorber	6.1	38.06
Compressor	4.908	30.62
Desorber	3.305	20.62
Solution heat exchanger	0.08433	0.5261
Solution pump	0.1124	0.7013
Expansion valve	1.519	9.474
Total	14.1287	100

Table III : Heat transfer rates of components and performance parameters of the system.

<b>Components</b>	<b>Heat Transfer rates (KW)</b>
Absorber	100
Desorber	73.17
Solution pump	0.001621
Compressor	25.24
<b>Performance parameters</b>	
Coefficient of performance (COP)	3.961
Circulation ratio (CR)	1.897
Exergetic efficiency	0.3747

Table IV : Variation of coefficient of performance with compressor efficiency at various desorber temperatures. ( $T_a = 60^\circ\text{C}$ ,  $\varepsilon = 0.7$ )

$\eta_c$	$T_d = 30^\circ\text{C}$	$T_d = 35^\circ\text{C}$	$T_d = 40^\circ\text{C}$
0.5	3.115	3.124	3.131
0.6	3.538	3.549	3.557
0.7	3.961	3.974	3.983
0.8	4.384	4.399	4.409
0.9	4.807	4.824	4.835
1	5.23	5.248	5.261

Table V : Exergetic efficiencies for various compressor efficiencies.

Absorber temperature (° C)	Exergetic efficiency		
	( $\eta_c = 0.6$ )	( $\eta_c = 0.7$ )	( $\eta_c = 0.8$ )
60	0.3186	0.3567	0.3948
65	0.3601	0.4028	0.4456
70	0.3903	0.4359	0.4815
75	0.4013	0.4467	0.492
80	0.3689	0.4068	0.4446

Table VI : Exergy destruction ratios of all the components expressed as percentages at various absorber temperatures.

Absorber temperature (°C)	EDR <sub>a</sub> (%)	EDR <sub>c</sub> (%)	EDR <sub>d</sub> (%)	EDR <sub>ev</sub> (%)	EDR <sub>p</sub> (%)	EDR <sub>shx</sub> (%)
60	38.22	28.1	23.31	9.519	0.5473	0.3046
65	38.97	30.04	17.47	11.21	0.9561	1.348
70	38.28	31.75	12.28	13	1.516	3.173
75	36.25	32.82	7.538	14.83	2.307	6.256
80	32.73	32.47	3.38	16.61	3.443	11.36

Table VII : Exergy destruction ratio of the compressor with absorber temperature at various compressor efficiencies.

<b>Absorber temperature(°C)</b>	<b>EDR<sub>c</sub> (<math>\eta_c = 0.7</math>)</b>	<b>(<math>\eta_c = 0.8</math>)</b>	<b>(<math>\eta_c = 0.9</math>)</b>	<b>(<math>\eta_c = 1</math>)</b>
60	28.1	19.97	10.63	0.00002576
65	30.04	21.58	11.62	0.00002852
70	31.75	23.01	12.51	0.00003105
75	32.82	23.88	13.04	0.00003256
80	32.47	23.5	12.75	0.00003161

Table VIII : Exergy destruction ratio of the absorber with absorber temperature.(  $T_d = 30^\circ\text{C}, 35^\circ\text{C}, 40^\circ\text{C}$ )

<b>Absorber temperature(°C)</b>	<b>EDR<sub>a</sub> (<math>T_d = 30^\circ\text{C}</math>)</b>	<b>EDR<sub>a</sub> (<math>T_d = 35^\circ\text{C}</math>)</b>	<b>EDR<sub>a</sub> (<math>T_d = 40^\circ\text{C}</math>)</b>
60	37.85	38.22	38.50
65	37.96	38.97	39.66
70	36.31	38.27	39.57
75	32.87	36.25	38.44
80	27.34	32.73	36.20

Table IX : Exergy destruction ratio of the desorber with absorber temperature.(  $T_d = 30^\circ\text{C}, 35^\circ\text{C}, 40^\circ\text{C}$ )

<b>Absorber temperature(<math>^\circ\text{C}</math>)</b>	<b><math>\text{EDR}_d (T_d = 30^\circ\text{C})</math></b>	<b><math>\text{EDR}_d (T_d = 35^\circ\text{C})</math></b>	<b><math>\text{EDR}_d (T_d = 40^\circ\text{C})</math></b>
60	20.24	23.31	25.84
65	14.09	17.47	20.29
70	8.633	12.28	15.39
75	3.88	7.537	10.87
80	0.4556	3.83	6.671

Table X : Exergy destruction ratio of the solution pump with absorber temperature.( $T_d = 30^\circ\text{C}, 35^\circ\text{C}, 40^\circ\text{C}$ )

<b>Absorber temperature(<math>^\circ\text{C}</math>)</b>	<b><math>\text{EDR}_p (T_d = 30^\circ\text{C})</math></b>	<b><math>\text{EDR}_p (T_d = 35^\circ\text{C})</math></b>	<b><math>\text{EDR}_p (T_d = 40^\circ\text{C})</math></b>
60	0.6994	0.5483	0.4407
65	1.262	0.9579	0.7512
70	2.071	1.519	1.16
75	3.27	2.311	1.715
80	5.058	3.449	2.484

Table XI : Exergy destruction ratio of the expansion valve with absorber temperature. ( $T_d = 30^\circ\text{C}, 35^\circ\text{C}, 40^\circ\text{C}$ )

<b>Absorber temperature(<math>^\circ\text{C}</math>)</b>	<b><math>\text{EDR}_{\text{ev}} (T_d = 30^\circ\text{C})</math></b>	<b><math>\text{EDR}_{\text{ev}} (T_d = 35^\circ\text{C})</math></b>	<b><math>\text{EDR}_{\text{ev}} (T_d = 40^\circ\text{C})</math></b>
60	9.918	9.519	9.172
65	11.71	11.21	10.79
70	13.61	13	12.47
75	15.67	14.83	14.18
80	17.54	16.61	15.86

Table XII : Exergy destruction ratio of the solution heat exchanger with absorber temperature. ( $T_d = 30^\circ\text{C}, 35^\circ\text{C}, 40^\circ\text{C}$ )

<b>Absorber temperature(<math>^\circ\text{C}</math>)</b>	<b><math>\text{EDR}_{\text{shx}} (T_d = 30^\circ\text{C})</math></b>	<b><math>\text{EDR}_{\text{shx}} (T_d = 35^\circ\text{C})</math></b>	<b><math>\text{EDR}_{\text{shx}} (T_d = 40^\circ\text{C})</math></b>
60	0.7878	0.3046	0.03849
65	2.477	1.348	0.6929
70	5.483	3.173	1.827
75	10.67	6.255	3.723
80	19.42	11.36	6.831

## REFERENCES

- [1] *Morawetz, E.*, “Sorption-compression heat pumps”, *International Journal of Energy Research.*, Vol.13, (1989), pp.83-102.
- [2] *Minea, V. and Chiriac, F.*, Hybrid absorption heat pump with ammonia/water mixture- Some design guidelines and district heating application”, *International Journal of Refrigeration*”, Vol. 29, (2006), pp. 1080-1091.
- [3] *Pourezza-Djourshari,S. and Radermacher R.*, “Calculation of performance of vapour compression heat pumps with solution circuits using the mixture R22-DEGDME.”, *Int J. Refrig.*, Vol.9, (1986), pp.245-250.
- [4] *Arun, M.B., Maiya, M.P. and Srinivasamurthy, S.*, “Optimization study of the compression/absorption cycle.”, *Int J. Refrig.*, Vol.14, (1991), pp.16-23.
- [5] *Brunnin., O., Feidt, M. and Hivet, B.*, “Comparison of the working domains of some compression heat pumps and a compression-absorption heat pump.”, *Int J. Refrig.*, Vol.20, (1997), pp.308-318.
- [6] *Ahlby, L., Hodgett, D. and Berntsson, T.*, “Optimization study of the compression/absorption cycle.”, *International Journal of Refrigeration*, Vol.14, (1991) pp.16-23.
- [7] *George, J. M., Marx, W. and Srinivasa Murthy, S.*, “Analysis of R22-DMF compression-absorption heat pump.”, *Heat recovery systems and CHP*, Vol.19 (1989) pp.433-446.
- [8] *Hulten, M. and Berntsson, T.*, “The compression/absorption heat pump cycle- conceptual design improvements and comparisons with the compression cycle.”,
- [9] *Hulten, M. and Berntsson, T.*, “The compression/absorption cycle- influence of some major parameters on COP and a comparison with the compression cycle.”, *Int J. Refrig.*, Vol.22, (1999), pp.91-106.

- [10] *Boer, D., Valles, M. and Coronas, A.*, “Performance of double effect absorption compression cycles for air conditioning using methanol-TEGDME and TFE-TEGDME systems as working pairs.”, *Int J. Refrig.*, Vol.21, (1998), pp.542-555.
- [11] *Pratihari, A.K., Kaushik, S.C. and Agarwal, R.S.*, “Thermodynamic Modeling and feasibility analysis of compression-absorption refrigeration system.”, *Emerging Technologies in air conditioning and refrigeration*, Acreconf 2001.
- [12] *Ferreira, C.A., Zamfirescu, C. and Zaytsev, D.*, “Twin screw oil free wet compressor for compression-absorption cycle”, *International Journal of Refrigeration*, Vol. 29, (2006), pp. 556-565
- [13] *Bourouis, M., Nogues, M., Boer, D. and Coronas, A.*, “Industrial heat recovery by absorption/compression heat pump using TFE-H<sub>2</sub>O-TEGDME working mixture”, *Applied thermal Engineering*, Vol. 20, (2000), pp. 355-369.
- [14] *Tarique, S.M. and Siddiqui, M.A.*, “Performance and economic study of the combined absorption/compression heat pump.”, *Energy conversion and management*, Vol.40, (1999), pp. 575-591.
- [15] *Kilic, M. and Kaynakli, O.*, “Second law based thermodynamic analysis of water-lithium bromide absorption refrigeration system”, *Energy*, Vol.32, (2007), pp. 1505-1512.
- [16] *Talbi, M.M. and Agnew, B.*, “Exergy analysis: an absorption refrigerator using lithium bromide and water as the working fluids”, *Applied Thermal Engineering*, Vol. 20, (2000), pp. 619-630.
- [17] *Arora, A. and Kaushik, S.C.*, “Theoretical analysis of a vapour compression refrigeration system with R502, R404A and R507A,” *International Journal of Refrigeration*, Vol. xxx, (2008), pp. 1-8.
- [18] *Gupta, A. and Das, S.K.*, “Second law analysis of crossflow heat exchanger in the presence of axial dispersion in one fluid”, *Energy*, Vol.32, (2007), pp.664-672.



- [19] *Rosen, A.M. and Scott, S.D.*, “Entropy production and Exergy Destruction: Part II-illustrative technologies”, *International Journal of Hydrogen Energy*, Vol. 28, (2003), pp. 1315-1323.
- [20] *Kaynakli O. and Yamankaradeniz R.*, “Thermodynamic analysis of absorption refrigeration system based on entropy generation”, Department of Mechanical Engineering, Faculty of Engineering and Architecture, Uludag University, Turkey.
- [21] *Rane, M.V. and Radermacher, R.*, “Experimental Investigation of a two stage Vapour compression heat pumps with solution circuits”, The University of Maryland, Department of Mechanical Engineering,
- [22] *Kairouani, L. and Nehdi, D.*, “Cooling performance and energy saving of a compression-absorption refrigeration system assisted by geothermal energy“, *Applied Thermal Engineering*, Vol.26, (2006), pp. 288-294.
- [23] *Fukuta, M., Yanagisawa, T., Iwata, H. and Tada, K.*, “Performance of compression/absorption hybrid refrigeration cycle with propane/mineral oil combination.”, *International Journal of Refrigeration*, Vol.25, (2002) pp.907-15.
- [24] *Engineering Equation Solver*, Academic Commercial Version, V 7.933 (07/13/07), f-Chart software, (2007), Education Version distributed by Mc Graw Hill.
- [25] *Zhou, Q. and Radermacher, R.* , “Development of a vapour compression cycle with a solution circuit and desorber/absorber heat exchange.”, *International Journal of Refrigeration*, Vol.20, (1997) pp.16-23.